

# Comparative Analysis of Transmembrane Regulators of the Filamentous Growth Mitogen-Activated Protein Kinase Pathway Uncovers Functional and Regulatory Differences

Hema Adhikari, Lauren M. Caccamise, Tanaya Pande, Paul J. Cullen

Department of Biological Sciences at the University at Buffalo, Buffalo, New York, USA

**Filamentous growth is a microbial differentiation response that involves the concerted action of multiple signaling pathways. In budding yeast, one pathway that regulates filamentous growth is a Cdc42p-dependent mitogen-activated protein kinase (MAPK) pathway. Several transmembrane (TM) proteins regulate the filamentous growth pathway, including the signaling mucin Msb2p, the tetraspan osmosensor Sho1p, and an adaptor Opy2p. The TM proteins were compared to identify common and unique features. Msb2p, Sho1p, and Opy2p associated by coimmunoprecipitation analysis but showed predominantly different localization patterns. The different localization patterns of the proteins resulted in part from different rates of turnover from the plasma membrane (PM). In particular, Msb2p (and Opy2p) were turned over rapidly compared to Sho1p. Msb2p signaled from the PM, and its turnover was a rate-limiting step in MAPK signaling. Genetic analysis identified unique phenotypes of cells over-expressing the TM proteins. Therefore, each TM regulator of the filamentous growth pathway has its own regulatory pattern and specific function in regulating filamentous growth. This specialization may be important for fine-tuning and potentially diversifying the filamentation response.**

Many fungal species undergo a growth response called filamentous growth, also referred to as invasive or pseudohyphal growth (1, 2). In some fungal pathogens, filamentous growth is required for virulence (3, 4). For example, *Candida albicans* is an opportunistic human pathogen that invades host tissues in the hyphal form (5). The budding yeast, *Saccharomyces cerevisiae*, differentiates from the yeast form to the filamentous form when environmental nutrients are limiting (6). Cells undergoing filamentous growth are composed of branched filaments of elongated and connected cells. This phenotype results from the reorganization of cell polarity, a delay in the G<sub>2</sub> phase of the cell cycle, and changes in the expression of cell-surface adhesion molecules (7–9).

Filamentous growth in yeast involves the concerted effort of multiple signal transduction pathways (10). Among the pathways that control filamentous growth are the RAS/cyclic AMP/protein kinase A pathway (11, 12), the target of rapamycin pathway (13), and a Cdc42p-dependent mitogen-activated protein kinase (MAPK) pathway, commonly referred to as the filamentous growth pathway (14, 15). The polarity establishment Rho (Ras homology) GTPase Cdc42p is a global regulator of cell polarity and signaling (16, 17) that regulates the filamentous growth pathway (18, 19). Cdc42p and its major activator, the guanine nucleotide exchange factor (GEF) Cdc24p are regulated in the filamentous growth pathway by the scaffold-type adaptor Bem4p (20). The active, GTP-bound conformation of Cdc42p associates with the p21-activated kinase (PAK) Ste20p (18, 19) to activate a canonical MAPK cascade (Ste11p-Ste7p-Kss1p [21]) that culminates in the phosphorylation/activation of transcription factors (Ste12p and Tec1p; including two newly identified factors Msa1p and Msa2p [22, 23]) which induce target genes that function to produce the filamentous cell type (24, 25).

Three transmembrane (TM) proteins regulate the filamentous growth pathway (Msb2p, Sho1p, and Opy2p). Msb2p and Opy2p are type I TM proteins, whereas Sho1p has four TM domains.

Msb2p is a member of the signaling mucin family of proteins (26, 27). Proteolytic processing in the glycosylated extracellular domain of Msb2p results in the release of an inhibitory glycodomain. This posttranslational modification is required for activation of the filamentous growth pathway (28). Underglycosylation of Msb2p's extracellular domain leads to elevated proteolytic processing by a mechanism that involves the unfolded protein response (29).

Sho1p also regulates the filamentous growth pathway (30, 31). Sho1p associates with Msb2p (30) and the GEF for Cdc42p, Cdc24p (28, 32). Opy2p also regulates the filamentous growth pathway (33–35). Opy2p interacts with an adaptor protein, called Ste50p, whose main function is to regulate the MAPKKK Ste11p (33, 34, 36–38). It is generally thought that Opy2p regulates the plasma membrane (PM) recruitment of Ste11p, thereby facilitating its activation by upstream regulators.

Many of the proteins that regulate the filamentous growth pathway also regulate other MAPK pathways in the same cell. For example, Msb2p (39, 40), Sho1p (41–44), and Opy2p (45, 46) also regulate the Ste11p branch of the high-osmolarity glycerol response (HOG) MAPK pathway. The HOG pathway is an osmo-

Received 15 May 2015 Accepted 17 June 2015

Accepted manuscript posted online 26 June 2015

Citation Adhikari H, Caccamise LM, Pande T, Cullen PJ. 2015. Comparative analysis of transmembrane regulators of the filamentous growth mitogen-activated protein kinase pathway uncovers functional and regulatory differences. *Eukaryot Cell* 14:868–883. doi:10.1128/EC.00085-15.

Address correspondence to Paul J. Cullen, pjcullen@buffalo.edu.

Supplemental material for this article may be found at <http://dx.doi.org/10.1128/EC.00085-15>.

Copyright © 2015, American Society for Microbiology. All Rights Reserved. doi:10.1128/EC.00085-15

TABLE 1 Yeast strains used in the study

Strain <sup>a</sup>	Genotype <sup>b</sup>	Source or reference
PC538	<i>MATa ste4 FUS1-lacZ FUS1-HIS3 ura3-52</i>	30
PC539	<i>MATa ste4 FUS1-lacZ FUS1-HIS3 ura3-52 ste12::KIURA3</i>	30
PC622	<i>MATa ste4 FUS1-lacZ FUS1-HIS3 ura3-52 PGAL-SHO1::KanMX6</i>	30
PC948	<i>MATa ste4 FUS1-lacZ FUS1-HIS3 ura3-52 msb2::KanMX6</i>	30
PC965	<i>MATa ste4 FUS1-lacZ FUS1-HIS3 ura3-52 msb2::KanMX6 sho1::KIURA3</i>	30
PC1083	<i>MATa ste4 FUS1-lacZ FUS1-HIS3 ura3-52 MSB2-HA PGAL-MSB2::KanMX6</i>	30
PC1508	<i>MATa ste4 FUS1-lacZ FUS1-HIS3 ura3-52 PGAL-ALY1::KanMX6</i>	This study
PC1531	<i>MATa ste4 FUS1-lacZ FUS1-HIS3 ura3-52 sho1::HYG</i>	30
PC1549	<i>MATa ste4 FUS1-lacZ FUS1-HIS3 ura3-52 SHO1-YFP::KanMX6</i>	This study
PC1658	<i>NY13 MATa ura3-52*</i>	120
PC1664	<i>NY412 MATa ura3-52 sec3-2*</i>	120
PC1702	<i>MATa ste4 FUS1-lacZ FUS1-HIS3 ura3-52 SHO1-HA::KanMX6</i>	30
PC2084	<i>MATa ste4 FUS1-lacZ FUS1-HIS3 ura3-52 MSB2-MYC::KanMX6</i>	This study
PC2094	<i>MATa ste4 FUS1-lacZ FUS1-HIS3 ura3-52 MSB2-GFP::KanMX6</i>	30
PC2680	<i>MATa ste4 FUS1-lacZ FUS1-HIS3 ura3-52</i>	This study
PC2622	<i>MATa ste4 FUS1-lacZ FUS1-HIS3 ura3-52 snf8::HYG</i>	91
PC3691	<i>MATa ste4 FUS1-lacZ FUS1-HIS3 ura3-52 MSB2-HA rim101::NAT</i>	This study
PC3752	<i>MATa ste4 FUS1-lacZ FUS1-HIS3 ura3-52 opy2::KIURA3</i>	35
PC4848	<i>MATa ste4 FUS1-lacZ FUS1-HIS3 ura3-52 pGAL-OPY2::KanMX6</i>	35
PC5596	<i>MATa ste4 FUS1-lacZ FUS1-HIS3 ura3-52 pGAL-OPY2- mCHERRY::KanMX6</i>	This study
PC5710	<i>MATa ste4 FUS1-lacZ FUS1-HIS3 ura3-52 MSB2 mCHERRY::KanMX6</i>	This study
PC5822	<i>MATa ste4 FUS1-lacZ FUS1-HIS3 ura3-52 vps27::KIURA3</i>	91
PC5824	<i>MATa ste4 FUS1-lacZ FUS1-HIS3 ura3-52 rim101-531::KIURA3</i>	This study
PC5828	<i>MATa ste4 FUS1-lacZ FUS1-HIS3 ura3-52 rim101-531::KIURA3 snf8::HYG</i>	This study
PC5831	<i>MATa ste4 FUS1-lacZ FUS1-HIS3 ura3-52 vps35::KIURA3</i>	91
PC5836	<i>MATa ste4 FUS1-lacZ FUS1-HIS3 ura3-52 MSB2-GFP at 1222 residues deleting 1223-1306::KanMX6</i>	This study
PC5838	<i>MATa ste4 FUS1-lacZ FUS1-HIS3 ura3-52 MSB2-GFP at 1238 residues deleting 1239-1306::KanMX6</i>	This study
PC5850	<i>MATa ste4 FUS1-lacZ FUS1-HIS3 ura3-52 MSB2-HA at 500 residues K1223R K1239R K1245R-GFP::KanMX6::KIURA3</i>	29
PC5983	<i>MATa ste4 FUS1-lacZ FUS1-HIS3 ura3-52 msb2::KanMX6 opy2::NAT</i>	This study
PC5984	<i>MATa ste4 FUS1-lacZ FUS1-HIS3 ura3-52 sho1::HYG opy2::NAT</i>	This study
PC6016 <sup>c</sup>	<i>MATa can1Δ::Ste2pr-spHIS5 lyp1Δ::Ste3pr-LEU2 his3::hisG leu2Δ0 ura3Δ0</i>	121
PC6319	<i>MATa ste4 FUS1-lacZ FUS1-HIS3 ura3-52 msb2::KIURA3 opy2::NAT sho1::HYG</i>	This study

<sup>a</sup> All strains are in the  $\Sigma$ 1278b background unless otherwise indicated.

<sup>b</sup> *KLURA3* refers to the *Kluyveromyces lactis URA3* cassette. \*, W303 background.

<sup>c</sup>  $\Sigma$ 1278b ordered deletion collection control strain *MATa can1Δ::Ste2pr-spHIS5lyp1Δ::Ste3pr-LEU2 his3::hisG leu2Δ0 ura3Δ*. Mutants from C. Boone  $\Sigma$ 1278b *MATa* deletion collection were used in the study.

sensing pathway that is composed of a Ste11p branch and a Sln1p-Ssk1p branch, which converge on the MAPKK Pbs2p and MAPK Hog1p. Although it is generally unclear how the same sensors regulate different pathways, it has been shown that a second signaling mucin, Hkr1p, regulates the HOG pathway (39) but not the filamentous growth pathway (47). Thus, it may be that the two signaling mucins primarily regulate different MAPK pathways. In a recent study, the interactions between the TM regulators of the HOG pathway were explored. Sho1p was found to function as an osmosensor by dynamically associating with Ste50p and with Hkr1p and Opy2p (44). Sho1p can oligomerize (48). Saito and coworkers showed that Sho1p forms oligomers of the dimers-of-trimers architecture. Osmolarity induces changes in this architecture, which leads to changes in Sho1p's interaction with Ste50p and HOG pathway activation through Hkr1p and Opy2p (44).

Studies of Sho1p and other regulators of the HOG pathway provoke questions about how the filamentous growth pathway might be regulated. Do Msb2p, Sho1p, and Opy2p function in a protein complex? Are the proteins coregulated in their delivery to the PM or turnover? Does each TM protein carry out the same function or do they have unique functions in regulating the filamentation response? These questions are generally interesting because many signal transduction pathways, like the protein kinase

C (PKC) (49, 50) and HOG pathways (46) in yeast and the epidermal growth factor receptor pathway in humans (51, 52), are regulated by multiple TM proteins. We examine here several regulatory and functional aspects of the proteins. We show that each protein has a unique cellular localization pattern and a unique rate of turnover. In addition, each protein has a unique phenotype when overexpressed. We suggest that the unique regulatory features that control each protein are important for proper activation of the filamentous growth pathway.

## MATERIALS AND METHODS

**Microbiological techniques.** Yeast and bacterial strains were manipulated by standard methods (53, 54). Yeast strains were grown in YEP media supplemented with 2% glucose (GLU [D]) or 2% galactose (GAL). All experiments were carried out at 30°C unless otherwise indicated. The mating-specific reporter *FUS1* was also used (55), which in cells lacking an intact mating pathway (*ste4Δ*), exhibits Msb2p- and filamentous growth/pathway-dependent expression (30). *FUS1-HIS3* expression was used to confirm results and was measured by spotting equal amounts of cells onto synthetic medium lacking histidine. The single cell invasive growth assay (56) and the plate-washing assay (14) were performed to evaluate filamentous growth.

**Strains and plasmids.** Yeast strains are described in Table 1. Overexpression constructs were obtained from an ordered collection obtained

from Open Biosystems (57). Gene disruptions and *GAL1* promoter fusions were made by PCR-based methods (58, 59) using plasmids provided by John Pringle (Stanford University). Some disruptions were created by the use of antibiotic resistant markers on cassettes HYG and NAT (60). Internal epitope fusions were created as described previously (61) using plasmids containing the 3×MYC and 3×HA epitopes. Integrations were confirmed by PCR analysis and phenotype.

Plasmid pRS316-SHO1-GFP (PC1601) was provided by Alan Davidson (University of Toronto) (62). Plasmid pGAL-SHO1<sup>D16H</sup>-GFP::KanMX6 was created by homologous recombination of the pGAL promoter into a strain containing pSHO1<sup>D16H</sup>-GFP, also provided by the Davidson lab. Plasmid pGAL-SHO1<sup>D16H</sup>-GFP KanMX6::NAT was created by homologous recombination of the NAT cassette in a strain harboring pGAL-SHO1<sup>D16H</sup>-GFP::KanMX6. pRS316 SHO1<sup>D16H</sup>-HA::KanMX6 URA3 (PC2432), pRS316 SHO1<sup>D16H</sup> P120L-HA::KanMX6, and pRS316 SHO1<sup>D16H</sup> S220F-HA::KanMX6 were made by homologous recombination-mediated replacement of the green fluorescent protein (GFP) epitope with the hemagglutinin (HA) epitope. pFLARE (fluorescent lipid-associated reporter) was provided by the Emr lab and contains the PH domain of PLC- $\delta$ . pFLARE was used as a control to detect PI(4,5)P2 at the PM (63).

*ALY1* was identified in a genetic screen using an inducible plasmid library (AYES library [64]). Plasmids were transformed into a wild-type strain (PC538), and >10,000 colonies were examined by replica plating from S-GAL-URA medium to S-GAL-URA-HIS medium to identify those that failed to express the *FUS1-HIS3* reporter and did not grow. The *ALY1* gene was identified by DNA sequencing, and its phenotype was confirmed by construction of p*GAL1-ALY1* in the genome.

**Protein localization.** Cyan fluorescent protein (CFP) and yellow fluorescent protein (YFP) variants of green fluorescent protein (GFP) were obtained from the yeast resource center (<http://depts.washington.edu/yeastrc/>), and fusion proteins were created by homologous recombination as described previously (65). Experiments that involved the hydrophilic dye FM4-64 were performed as described previously (66). Cells were grown to saturation in selective medium to maintain plasmids harboring fusion proteins. Cells were harvested by centrifugation and resuspended in YEPD medium for 4.5 h. FM4-64 was added to cells, and after 0.5 h of incubation at 30°C, cells were harvested, washed three times in water, and visualized by fluorescence microscopy at ×100.

**Protein turnover.** Analysis of protein turnover was determined in two ways. A pGAL-promoter shutoff experiment was performed as described previously (29). Cells were grown in YEP-GAL media for 4 h and transferred to YEPD media for the indicated time points. For the cycloheximide chase experiments cells were grown in YEP-GAL media for 4.5 h and treated with 25  $\mu$ g of cycloheximide/ml for the indicated time points.

**Immunological techniques.** Immunoblots were performed as described previously (28). Proteins were separated by SDS-PAGE on 10% gels (Bio-Rad, Hercules, CA) and transferred to nitrocellulose membranes (Protran BA85; VWR International, Inc., Bridgeport, NJ). Membranes were incubated in blocking buffer (5% nonfat dry milk, 10 mM Tris-HCl [pH 8], 150 mM NaCl, 0.05% Tween 20) for 1 h at 25°C. ECL-Plus immunoblotting reagents were used to detect secondary antibodies (Amersham Biosciences, Piscataway, NJ). Nitrocellulose membranes were incubated for 18 h at 4°C in blocking buffer containing a mouse monoclonal antibody against HA (12CA5; Roche Diagnostics) or a mouse monoclonal IgG antibody against GFP (Roche Diagnostics). Phosphorylated Kss1p was detected as described previously (67).

**Co-IP analysis.** Coimmunoprecipitation (co-IP) analysis was performed as described previously (68). To assess the interaction between Msb2p and Opy2p, wild-type (untagged [PC538]) and Msb2p-MYC (PC2084) strains expressing pOpy2p-GFP were grown for 16 h in SD-URA medium and subcultured in YEPD medium for 6 h. For the co-IPs, the expression of proteins was driven by their endogenous promoters. Cell lysates were immunoprecipitated with anti-GFP monoclonal antibodies (Rockland Scientific International, goat anti-GFP 600-101-215 antibody)

and examined by immunoblot analysis using anti-GFP (mouse anti-GFP [Roche Diagnostics], clones 7.1 and 13.1, catalog no. 11814460001) and anti-MYC antibodies (Delta Biolabs, catalog no. DB098). To assess the interaction between Sho1p and Opy2p, wild-type (PC538) and Sho1p-HA (PC1702) strains expressing pOpy2p-GFP were grown for 16 h in SD-URA and subcultured in YEPD medium for 6 h. Cell lysates were immunoprecipitated with polyclonal HA antibodies and examined by immunoblot analysis with anti-HA monoclonal antibodies and anti-GFP monoclonal antibodies described above. Cells grown to mid-log phase in YEPD were frozen as cell pellets at  $-80^{\circ}\text{C}$ . For each co-IP, the cells were thawed in 1× phosphate-buffered saline (PBS) and immunoprecipitation buffer (50 mM Tris [pH 8.0], 1 mM EDTA, 50 mM NaCl, 3% NP-40, 1 mM phenylmethylsulfonyl fluoride, 1× protease inhibitor cocktail [Roche, catalog no. 11836170001]), lysed using Fast Prep (FP120; Thermo Electronic Incorporation) three times for 32 s each time at a speed of 6.5 ms, and centrifuged at 13,000 rpm for 10 min. The cell lysate was pre-cleared with protein G-beads (Thermo Scientific, catalog no. 20398) for 30 min at 4°C by end-over-end rotation. Precleared lysates were centrifuged at 13,000 rpm for 10 min. The supernatants were incubated with antibodies for 2 h at 4°C. Washed protein G-beads were added, followed by incubation for 2.5 h at 4°C by end-over-end rotation. The beads were washed four times with 1 ml of immunoprecipitation buffer. Then, 2× SDS-PAGE buffer containing 2%  $\beta$ -mercaptoethanol was added, and the extracts were boiled with intermittent vortexing. Proteins were separated by SDS-PAGE for immunoblot analysis.

**Protein localization and microscopy.** The localization of Msb2p was examined using plasmids pGFP-Msb2p and pHA-Msb2p-GFP. For other experiments, a strain containing a genomic copy of Opy2p-mCherry and pMsb2p-GFP was used. Strains with genomic copies of Msb2p-mCherry and Opy2p-mCherry under the control of their native promoters harboring a pSho1p-GFP were used for colocalization studies. To assess the interdependence of localization patterns, wild type, *msb2 $\Delta$  sho1 $\Delta$* , *msb2 $\Delta$  opy2 $\Delta$* , and *sho1 $\Delta$  opy2 $\Delta$*  cells expressing pOpy2p-GFP, pSho1p-GFP and pHA-Msb2p-GFP were examined. Wild-type cells were used as a reference strain. Wild-type and *sec3-2* cells harboring pSho1p-GFP and pOpy2p-GFP were examined by fluorescence microscopy. For localization experiments involving the *sec3-2* mutant, cells were grown in SD-URA for 16 h at 30°C, shifted to 37°C for 4 h, and examined on a stage heated to 37°C.

Differential interference contrast and fluorescence microscopy using rhodamine, fluorescein isothiocyanate, YFP, and CFP filter sets were performed using an Axioplan 2 fluorescence microscope (Zeiss) with a Plan-Apochromat ×100/1.4 (oil) objective (NA 0.17). Digital images were obtained with the Axiocam MRM camera (Zeiss). Axiovision 4.4 software (Zeiss) was used for image acquisition and analysis and for rendering 3D Z-stack images. Images were further analyzed in Adobe Photoshop, where adjustments of brightness and contrast were made.

## RESULTS

**Msb2p, Sho1p, and Opy2p interact and regulate the filamentous growth pathway.** Three TM proteins (Msb2p, Sho1p, and Opy2p) regulate the filamentous growth pathway (Fig. 1A). Msb2p has previously been shown to interact with Sho1p (30). In addition, the processed form of Msb2p, called Msb2<sup>p</sup>, and Sho1p associate (28, 39). The interaction between Msb2p and Sho1p is required to induce a downstream signal (39). Opy2p also regulates the filamentous growth pathway (33, 34, 36, 38, 69), but whether Opy2p associates with Msb2p or Sho1p has not been examined in the context of the filamentous growth pathway. Opy2p is glycosylated and migrates as multiple bands by SDS-PAGE analysis (34). Co-IP analysis showed that Opy2p-GFP, which migrates at 65 kDa and at 75 and 100 kDa, interacted with Msb2<sup>p</sup>-Myc (Fig. 1B, left panel). Msb2<sup>p</sup>-Myc migrates at 45 kDa and as a larger form at ~75 kDa.

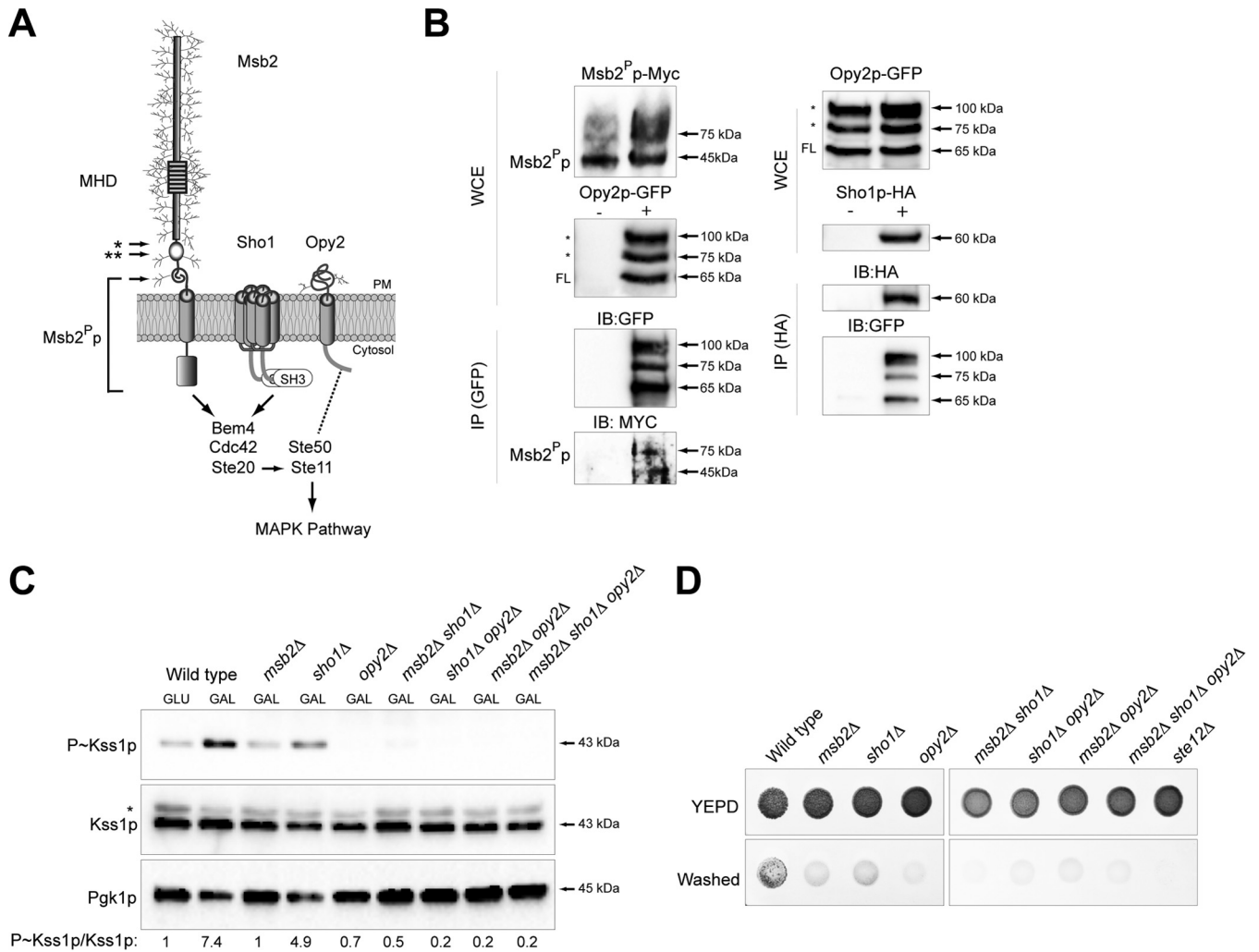


**FIG 1** TM regulators of the filamentous growth pathway interact and regulate the filamentous growth pathway. (A) Schematic representation of the pathway components (transmembrane and cytosolic) of the filamentous growth pathway. (B) Co-IP analysis. Left, Msb2<sup>P</sup>p-MYC and Opy2p-GFP associate by co-IP analysis. Right, Sho1p-HA and Opy2p-GFP associate by co-IP analysis. FL refers to full-length Opy2p, asterisks refer to presumptive glycosylated versions of the protein, as reported previously (34). (C) Phosphorylated Kss1p levels in the *msb2Δ*, *sho1Δ*, and *opy2Δ* single mutants and the indicated double and triple mutant combinations in YEP-GAL media. (D) Plate-washing assay showing agar invasion of the indicated strains. Plates were incubated for 48 h, photographed, washed in a stream of water, and photographed again.

Opy2p-GFP also associated with Sho1p-HA (Fig. 1B, right panel). Thus, Msb2p, Sho1p, and Opy2p associate with each other.

To assess the roles the TM proteins play in regulating the filamentous growth pathway, double and triple mutant combinations were tested. The activity of the filamentous growth pathway was assessed by phosphorylation of the MAPK Kss1p (P~Kss1p). We compared the *msb2Δ*, *sho1Δ*, and *opy2Δ* single mutants, the *msb2Δ sho1Δ*, *sho1Δ opy2Δ*, and *msb2Δ opy2Δ* double mutants, and the *msb2Δ sho1Δ opy2Δ* triple mutant. Strains were grown in the nonpreferred carbon source galactose, which activates the filamentous growth pathway (35) and promotes filamentous growth (56). As previously reported (30, 35), each single mutant showed a defect in P~Kss1p levels (Fig. 1C). The *msb2Δ* and *sho1Δ* mutants showed a less severe defect than the *opy2Δ* mutant. The *msb2Δ sho1Δ* double mutant showed a more severe defect than either single mutant. Other double-mutant combinations and the *msb2Δ sho1Δ opy2Δ* triple mutant showed a full reduction in

P~Kss1p levels. Similar results were observed by the plate-washing assay that measures invasive growth (Fig. 1D). These results indicate that Msb2p and Sho1p together contribute to Opy2p-dependent activation of the filamentous growth pathway. This idea is consistent with the prevailing view from our lab (70) and supports the interpretation of Msb2p and Sho1p function in the HOG pathway (39).

**Msb2p, Sho1p, and Opy2p have different localization patterns.** The fact that Msb2p, Sho1p, and Opy2p interact suggests that the proteins may be coregulated. The localization patterns of the three proteins were compared. The localization of Msb2p, Sho1p, and Opy2p has been examined. Each protein is localized at the PM (28, 30, 37, 39, 41, 42). However, differences in the localization patterns of the proteins have also been reported. For example, Sho1p is mainly found in buds (41, 42, 47), whereas Msb2p is mainly found in the vacuole (28, 29). To better address this question, colocalization experiments were performed. C-terminal

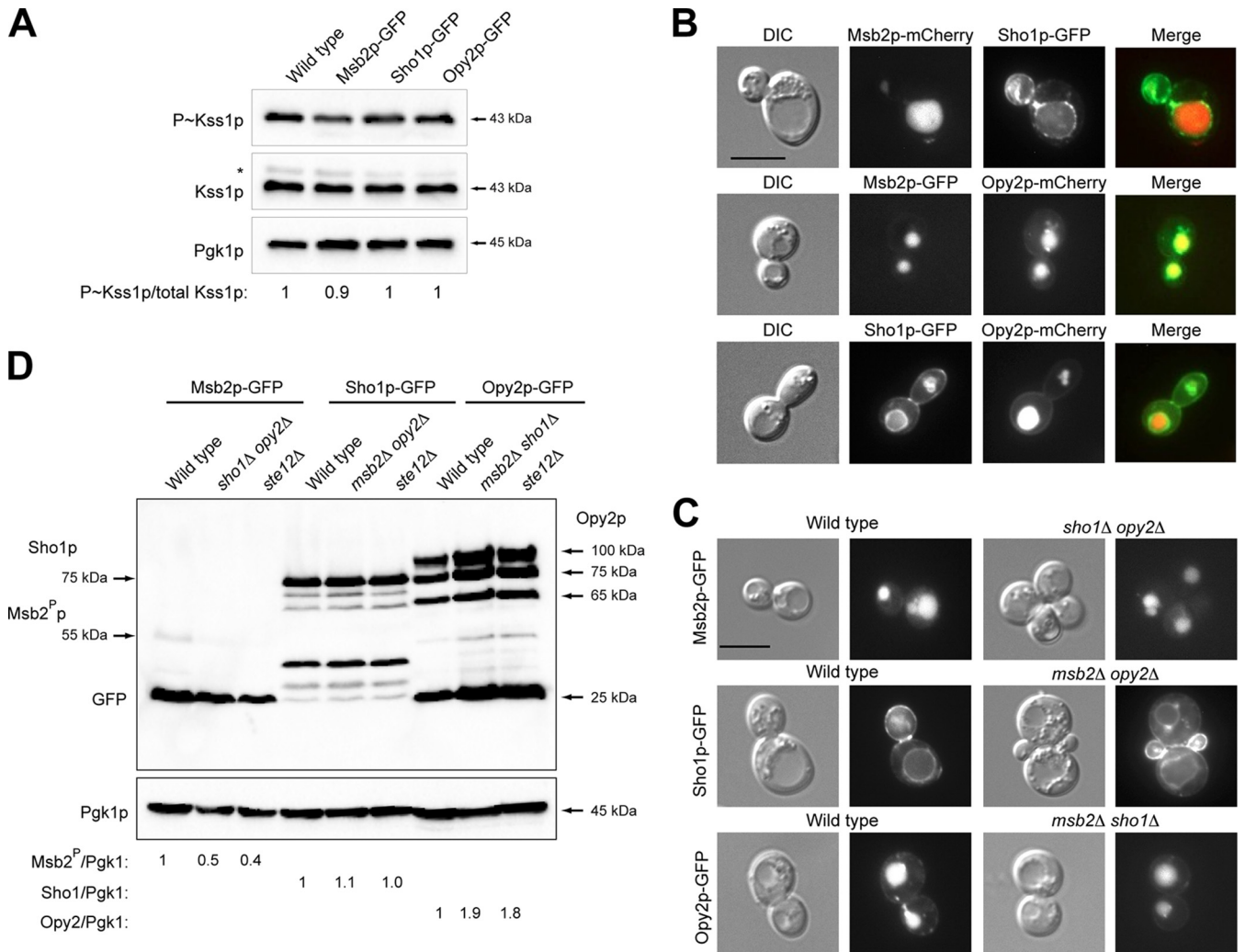


**FIG 2** The localization and steady-state levels of TM proteins that regulate the filamentous growth pathway. (A) The Msb2p-, Sho1p-, and Opy2p-GFP fusion proteins are functional based on P~Kss1p analysis. (B) Colocalization of TM regulators. Cells containing the indicated fusion proteins were grown in YEPD medium for 6 h and examined by fluorescence microscopy at  $\times 100$ . Scale bar, 5  $\mu$ m. (C) Localization of Msb2p, Sho1p, and Opy2p in the indicated mutants. Bar, 5  $\mu$ m. (D) Steady-state protein levels of Msb2p, Sho1p, and Opy2p in the indicated mutants. Msb2<sup>P</sup>p is a different size (55 kDa) than Fig. 1B because different epitope tags were used.

fusions to the proteins were functional based on P~Kss1p analysis (Fig. 2A). Colocalization experiments showed that Msb2p-mCherry was mainly present in the vacuole (Fig. 2B), whereas Sho1p-GFP was mainly at the PM and membranes surrounding internal compartments. Opy2p-mCherry and Msb2p-GFP colocalized in the vacuole. However, Opy2p-mCherry was also detected at the PM. The localization of Msb2p and Opy2p in the lumen of the vacuole, and Sho1p, which can also be seen in the vacuole to various degrees, probably represents build up of the cleaved form of GFP (see Fig. S1 in the supplemental material). Therefore, Msb2p, Sho1p, and Opy2p show overlapping and non-overlapping localization patterns.

Proteins that interact in a complex can influence the localization and stability of other members of the complex. The interdependency of TM regulators of the filamentous growth pathway was examined. Msb2p-GFP was not mislocalized in the *sho1Δ opy2Δ* double mutant (Fig. 2C). Sho1p-GFP was not mislocalized in the *msb2Δ opy2Δ* double mutant, and Opy2p-

GFP was not mislocalized in the *msb2Δ sho1Δ* double mutant. Therefore, the localization patterns of the TM regulators do not show interdependency. Steady-state protein levels were also compared. Immunoblot analysis showed that the level of Sho1p-GFP (in mid-log-phase cells) was not reduced in cells lacking Msb2p and Opy2p (Fig. 2D). However, the level of Msb2p-GFP was reduced in cells lacking Sho1p and Opy2p. This might be due to positive feedback, because expression of the *MSB2* gene is regulated by the filamentous growth pathway, specifically by the transcription factor Ste12p (30). In line with this possibility, the level of Msb2<sup>P</sup>p-GFP, but not Sho1p-GFP or Opy2p-GFP, was reduced in cells lacking the transcription factor Ste12p (Fig. 2D). The level of Opy2p-GFP was not reduced in cells lacking Sho1p and Msb2p. In fact, a minor increase in Opy2p levels was seen in some mutants, but this phenotype was not explored further. Therefore, although the TM regulators of the filamentous growth pathway associate, each

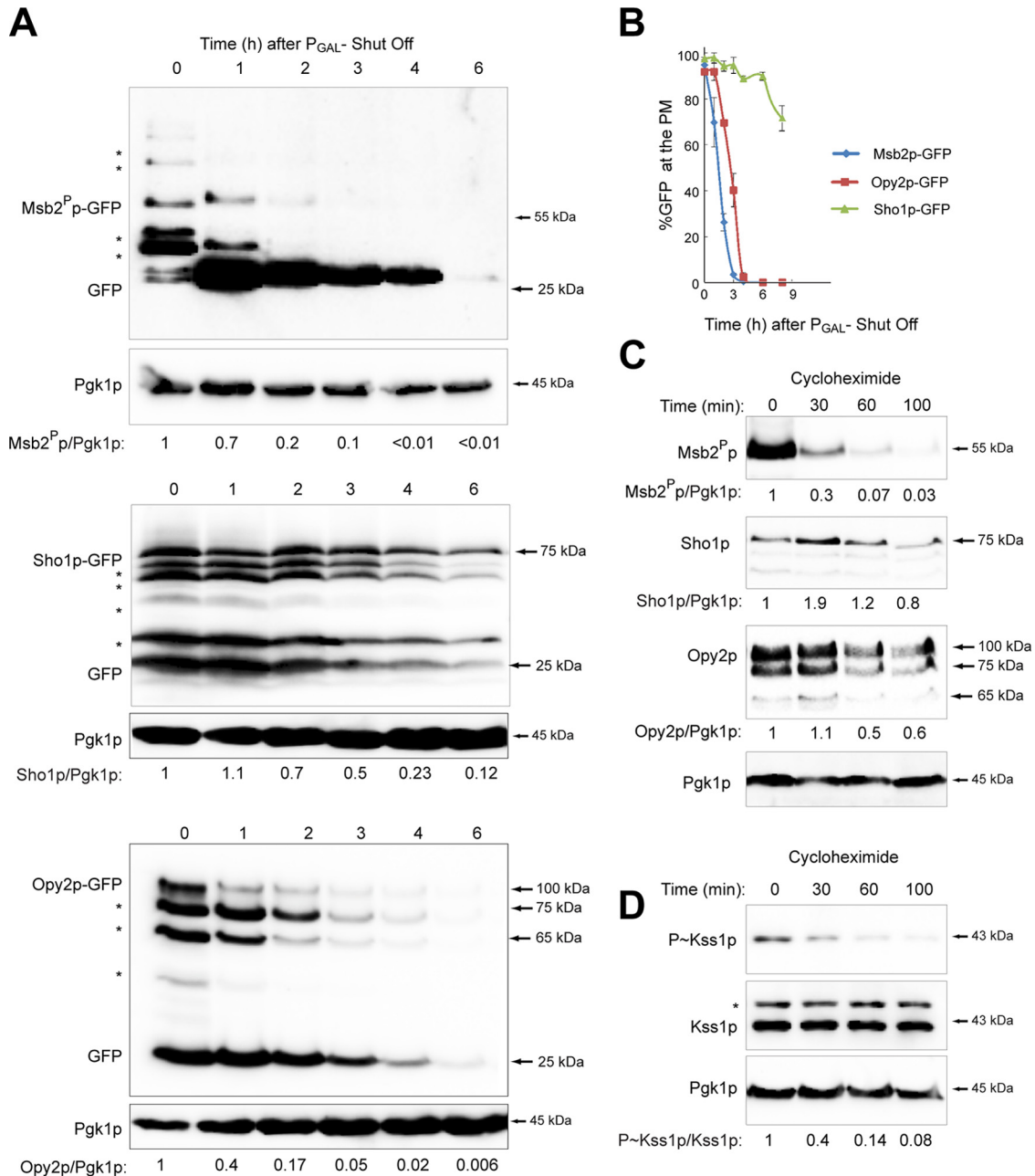


**FIG 3** Turnover of the Msb2p, Sho1p, and Opy2p proteins. (A) Proteins driven by the  $pGAL1$  promoter were examined at the indicated time points after shift to YEPD medium. Pgk1p, loading control for total protein levels. (B) Determination of GFP fluorescence (%) of Msb2p-GFP, Sho1p-GFP, and Opy2p-GFP at the plasma membrane by  $pGAL1$  promoter shutoff at the indicated time points. (C) Determination of protein levels of Msb2p-GFP, Sho1p-GFP, and Opy2p-GFP in YEP-GAL media after treatment with cycloheximide for the indicated time points. (D) Phosphorylated Kss1p levels in YEP-GAL media after treatment with cycloheximide for the indicated time points.

protein has a unique localization pattern that is independent of the other TM regulators of the pathway.

**Msb2p, Sho1p, and Opy2p have different rates of turnover from the PM.** The different localization patterns of the TM proteins may result from differences in turnover from the PM. The turnover of Sho1p, Msb2<sup>P</sup>p, and Opy2p was assessed by two methods. In one approach, functional GFP-tagged versions of the proteins were expressed under the control of the galactose-inducible  $GAL1$  promoter, and protein levels were examined at times after

promoter shut off, by shifting cells to glucose-rich medium. This experiment showed that Msb2<sup>P</sup>p-GFP was rapidly turned over, a finding consistent with a previous report (29) (Fig. 3A, top panel). The turnover of another Msb2p fusion protein (Msb2p-MYC) showed an equivalent turnover rate (see Fig. S2A in the supplemental material). In comparison, Sho1p was turned over more slowly (Fig. 3A, middle panel). Opy2p was turned over at an intermediate rate (Fig. 3A, bottom panel). The actual turnover rates might be different than indicated because they do not account for

the translation, trafficking, and PM delivery that occurs after promoter shutoff. To take this into account, the protein synthesis inhibitor cycloheximide (71) was also used to measure protein stability. Cycloheximide-chase experiments gave similar results (Fig. 3C). Based on the cycloheximide experiment, the half-life of Msb2<sup>P</sup> was <30 min, while that for Opy2p was ~30 min, and that for Sho1p was >100 min.

The different turnover rates of the TM proteins might account for their different localization patterns (Fig. 2B). To test this possibility, protein localization at the PM was assessed by fluorescence microscopy following promoter shutoff. Msb2p-GFP was cleared from the PM slightly faster than Opy2p-GFP (Fig. 3B). Both proteins were cleared from the PM more rapidly than Sho1p. Thus, the different turnover rates of the proteins from the PM can explain to some degree their different localization patterns.

The turnover of Msb2p might be impacted by endocytosis of the protein from the PM. The turnover of Msb2p was delayed in *end3Δ* and *end5Δ* mutants, based on immunoblot data (see Fig. S2B in the supplemental material) and localization of Msb2p-GFP in these mutants (see Fig. S2C in the supplemental material). The turnover of Msb2p was not severely impacted in the *sla1Δ* mutant, which regulates turnover of Wsc1p by its NFPXD motif (72). Msb2p, Sho1p, and Opy2p do not have an NFPXD motif; thus, their endocytosis occurs by a different mechanism.

The turnover of Msb2<sup>P</sup> from the PM might be a rate-limiting step in the attenuation of MAPK signaling. As shown above, Msb2<sup>P</sup> is turned over more rapidly than Sho1p or Opy2p. Moreover, a version of Msb2p with mutations in its turnover domain, Msb2p<sup>3KR</sup>, shows elevated MAPK activity (see Fig. S2E in the supplemental material) (29). Msb2p<sup>3KR</sup> was more stable than wild-type Msb2p after cycloheximide treatment (see Fig. S2D in the supplemental material). Likewise, a version of Msb2p lacking the turnover domain showed PM localization (29) (see Fig. S2E, 1-1222, in the supplemental material). Another way to test this possibility is to assess the activity of the filamentous growth pathway after treatment with cycloheximide. The activity of the filamentous growth pathway was reduced within 30 min of treatment with cycloheximide (Fig. 3D), which corresponded to the turnover rate of Msb2<sup>P</sup> (Fig. 3C). In comparison, the level of the Kss1p protein itself was not reduced. Multiple proteins regulate the filamentous growth pathway (Cdc24p, Cdc42p, Bem4p, Ste20p, Ste11p, Ste50p, Ste7p, Ste12p, and Tec1p). Turnover of any one of these proteins might be rate limiting, and we have not explored this possibility further. However, from the perspective of the TM proteins, turnover of Msb2<sup>P</sup> may be the rate-limiting step in attenuation of the filamentous growth pathway.

**Differential turnover of Msb2p, Opy2p, and Sho1p by ESCRT (endosomal sorting complex required for transport).** Many receptors are internalized by endocytosis and delivered by vesicular trafficking to the lysosome/vacuole, where they are degraded by proteases (73–75). In yeast, the vacuolar protease Pep4p functions to degrade proteins that are delivered to the vacuole (76). In the *pep4Δ* mutant, the levels of Msb2<sup>P</sup>-GFP, Opy2p-GFP, and Sho1p-GFP were present at elevated levels (see Fig. S1 in the supplemental material). Therefore, the proteins are delivered to and turned over in the vacuole.

Proteins are delivered to the vacuole for turnover in the late endosome. The ESCRT complex is responsible for delivery of proteins from the endosome to the vacuole (77, 78). In ESCRT mutants, proteins destined for the vacuole/lysosome accumulate in

the late endosome, also referred to as the multivesicular body (MVB [79, 80]). As expected from previous work (29), Msb2p-GFP accumulated in the MVB in ESCRT mutants, including the *snf8Δ* mutant (see Fig. S3A in the supplemental material) and other ESCRT mutants (see Fig. S3B). Opy2p showed a similar pattern (see Fig. S3A in the supplemental material). By comparison, Sho1p did not localize to the MVB (see Fig. S3A). To better resolve these patterns, cells were stained with the lipophilic dye FM4-64 (81). Msb2p-GFP and FM4-64 showed colocalization in the MVB in the *snf8Δ* mutant (Fig. 4A), whereas Sho1p-GFP localized to the PM. In fact, in the *snf8Δ* mutant, Sho1p-GFP could be detected in some cells (<5%) at multiple sites (Fig. 4A, arrows). Therefore, based on the localization data, Msb2p and Sho1p are delivered to the vacuole in different ways.

The turnover of some receptors is facilitated by ligand binding (82–86). A pool of inactive Sho1p may reside at the PM that, when activated, leads to elevated turnover. To test this possibility, a hyperactive allele of Sho1p, Sho1p<sup>P120L</sup> (28, 39), was examined. Sho1p<sup>P120L</sup> localized to internal compartments (Fig. 4, A and C). Steady-state Sho1p<sup>P120L</sup> protein levels were lower than wild-type Sho1p (Fig. 4B). We had previously reported that a version of Sho1p lacking its SH3 domain was localized to the PM (47) (Fig. 4C). However, cycloheximide experiments showed that Sho1p<sup>P120L</sup> protein was turned over at the same rate as that of the wild type (see Fig. S3C in the supplemental material). Thus, Sho1p<sup>P120L</sup> may be sequestered in an internal compartment rather than turned over at an elevated level. We also found that wild-type Sho1p-GFP showed an altered banding during growth in galactose (see Fig. S4 in the supplemental material), a stimulus that activates the filamentous growth pathway (35). Because Sho1p showed this pattern in an *msb2Δ opy2Δ* mutant (see Fig. S4 in the supplemental material), it may be an Msb2p and Opy2p-independent modification.

**Msb2p shows normal filamentous growth pathway activity in ESCRT mutants.** Some receptors that are turned over from the PM continue to signal from endosomes (87). Addressing this question for Msb2p is complicated because mutants in the ESCRT pathway (ESCRT-I, -II, and -III complexes) also impair the Rim101 pathway, which regulates the filamentous growth pathway (88). This connection between ESCRT and Rim101 extends to other fungal species (Fig. 5A) (89, 90). To dissect the different roles of Rim101 and ESCRT in impacting the filamentous growth pathway, mutants were examined that were compromised for Rim101 (*rim101Δ*), ESCRT (*vps27Δ*), or both (*snf8Δ*). The plate-washing assay showed that the *rim101Δ* and *snf8Δ* mutants were defective for invasive growth, whereas the *vps27Δ* mutant was not (Fig. 5B, washed). This indicates that the Rim101 pathway (but not ESCRT) impacts the activity of the filamentous growth pathway. Likewise, the *snf8Δ* and *rim101Δ* mutants (but not the *vps27Δ* mutant) were defective for MAPK signaling based on the activity of the *FUS1-HIS3* growth reporter (Fig. 5B, SD-HIS), which in  $\Sigma$ 1278b *ste4Δ* strains provides a readout of the filamentous growth pathway (91). Msb2p-GFP localized to the MVB in the *vps27Δ* and *snf8Δ* mutants but not the *rim101Δ* or *ste12Δ* mutants (Fig. 5C). Therefore, trapping Msb2p in the MVB in ESCRT mutants does not impact MAPK signaling. The *vps27Δ* mutant showed a minor defect in invasive growth by the plate-washing assay and a morphological defect by the single cell assay, which may reflect a minor role for ESCRT in regulating the filamentous growth response.

To further examine this question, the C-terminal domain of

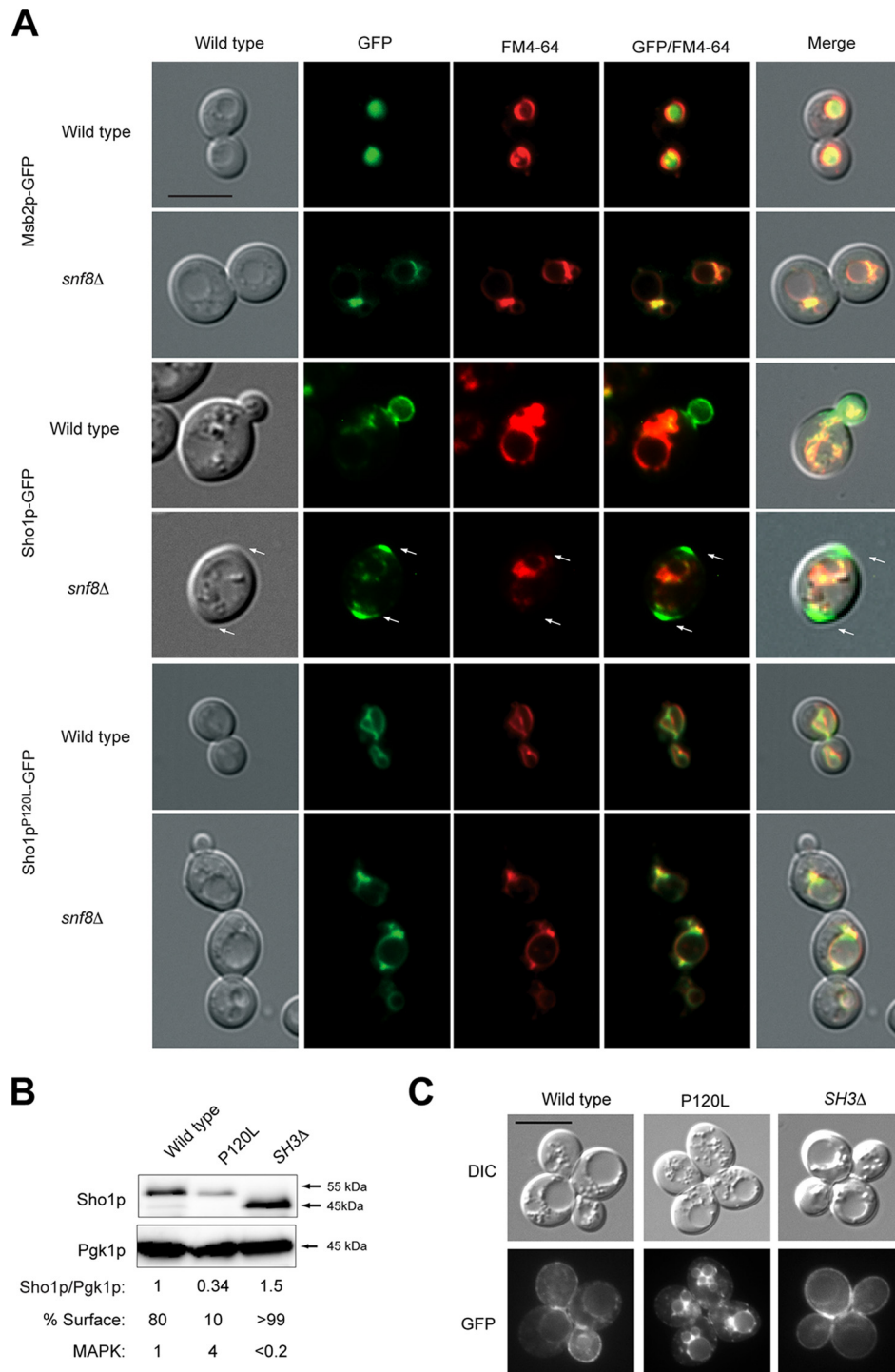


**FIG 4** Role of the ESCRT complex in regulating the trafficking of Msb2p and other PM regulators of the filamentous growth pathway. (A) Localization of Msb2p-GFP, Sho1p-GFP, and Sho1p<sup>P120L</sup>-GFP in wild-type cells and the *snf8Δ* mutant. Cells were costained with the membrane-specific dye FM4-64 to visualize the vacuole and associated compartments. Bar, 5  $\mu$ m. Arrows, Sho1p-GFP at multiple sites. (B) Immunoblot showing protein levels of Sho1p<sup>SH3Δ</sup>-GFP, Sho1p<sup>P120L</sup>-GFP and Sho1p-GFP fusions in wild-type cells. Pgk1p was used as a loading control. (C) Localization of Sho1p<sup>SH3Δ</sup>-GFP, Sho1p<sup>P120L</sup>-GFP, and Sho1p-GFP fusions in wild-type cells.

Rim101p was deleted, which leads to a constitutively active version of the protein (92). *RIM101-531* partially rescued the invasive growth (Fig. 5D, washed) and MAPK signaling defects of the *snf8Δ* mutant (Fig. 5D, SD-HIS). Furthermore, the *RIM101-531 snf8Δ*

double mutant showed Msb2p in the MVB (Fig. 5C). The single cell assay showed that *RIM101-531* was hyperfilamentous and bypassed the filamentation defects of the *snf8Δ* mutant (Fig. 5E). The major conclusion drawn from these experiments is that the signal-



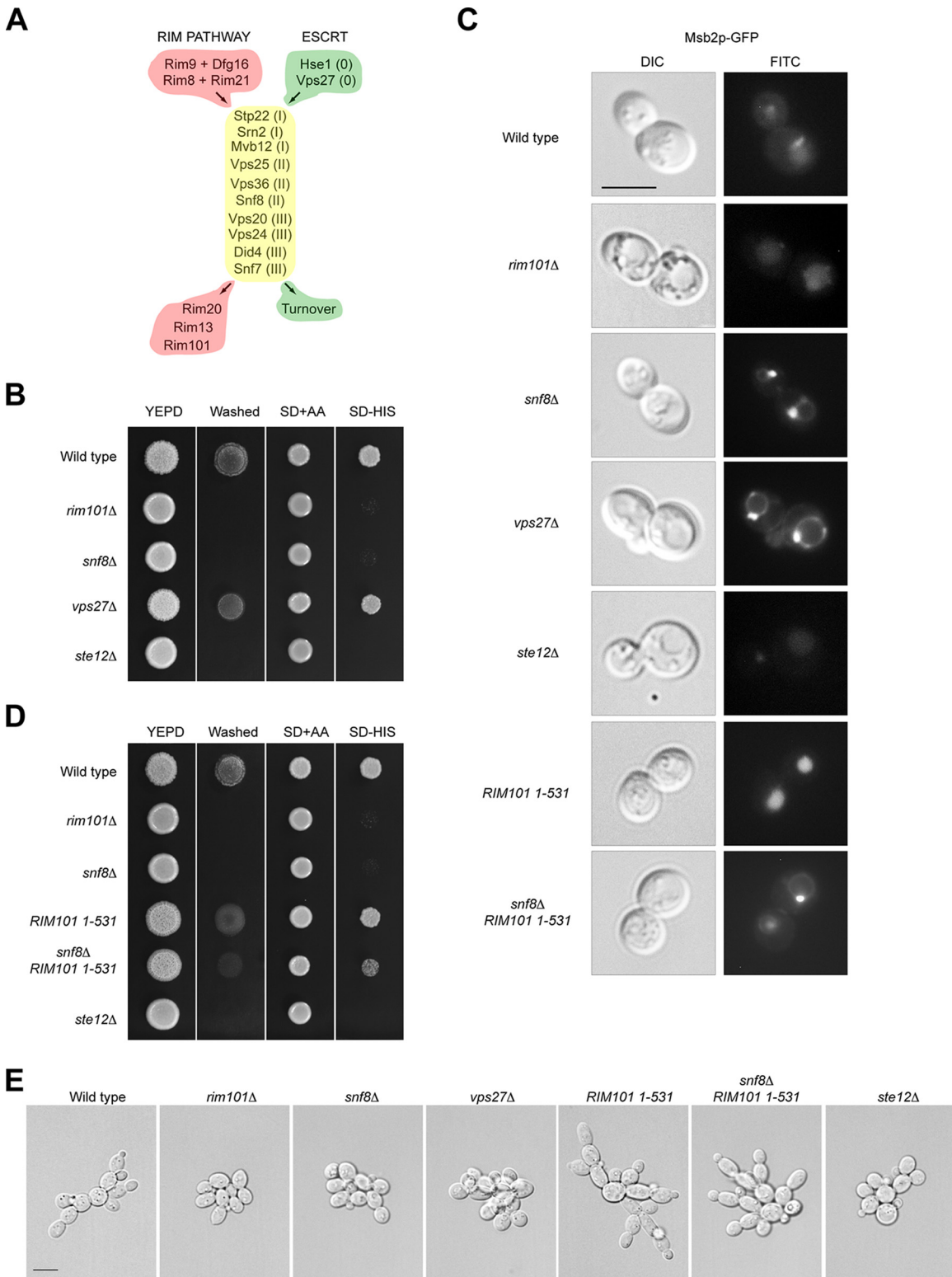


**FIG 5** Dissecting the roles of ESCRT and Rim101 in regulating the filamentous growth pathway. (A) Rim101 and ESCRT pathways. Overlapping proteins are shown in yellow, Rim101 pathway-specific components are shown in red, and ESCRT-specific proteins are shown in green. (B) On the left, plate-washing assay of the wild type, *rim101Δ*, *snf8Δ*, *vps27Δ* and *ste12Δ* mutants on YEPD media. The plates were incubated for 48 h, photographed, washed in a stream of water, and photographed again. On the right, the MAPK activity was assessed by the *FUS1-HIS3* growth reporter. Wild-type cells and the mutants were spotted on SD+AA and SD-His media. (C) Localization of Msb2p-GFP in wild-type cells and the indicated mutants. Cells were grown on YEPD media for 24 h. Cells were resuspended in water and evaluated by fluorescence microscopy at  $\times 100$ . Bar, 5  $\mu$ m. (D) Wild-type, *rim101Δ*, *snf8Δ*, *RIM101 1-531*, *RIM101 1-531 snf8Δ*, and *ste12Δ* cells were evaluated by a plate-washing assay and growth reporter assays as described in panel B. (E) Single-cell invasive growth assay. Cells were incubated for 24 h on S-GLU media. Representative cells are shown. Bar, 5  $\mu$ m.

Downloaded from http://ec.asm.org/ on March 16, 2016 by STATE UNIV NY AT BUFFALO

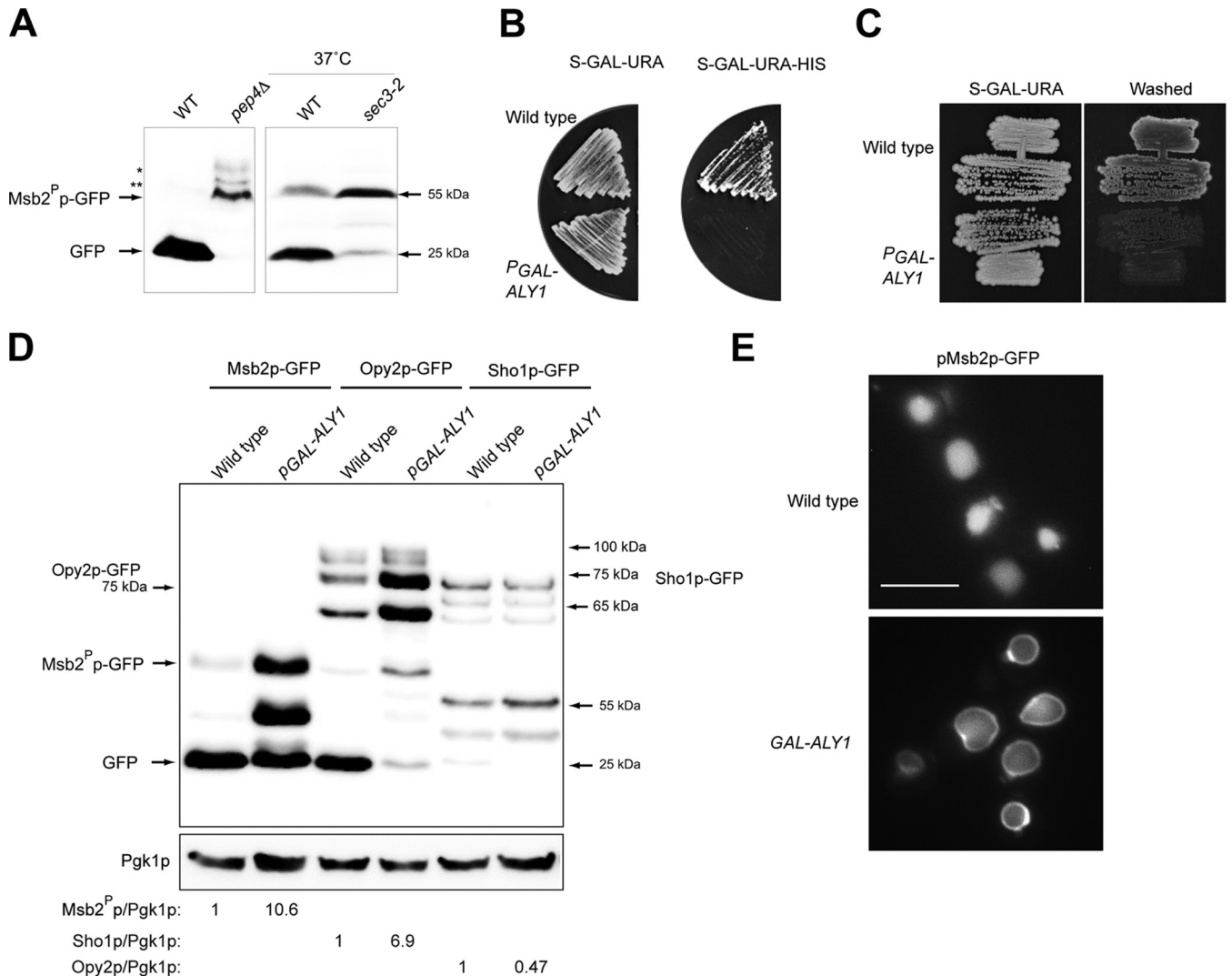


**FIG 6** Localization of Msb2p affects protein degradation and MAPK activity. (A) Immunoblot showing Msb2<sup>p</sup>-GFP and GFP levels in a *pep4Δ* mutant and *sec3-2* mutant at nonpermissive temperature. (B) *FUS1-HIS3* reporter assay of wild-type cells transformed with *pGAL-ALY1*. (C) Plate washing assay of wild-type cells transformed with *pGAL-ALY1* on S-GAL-URA media. (D) Immunoblot against GFP in Msb2p-GFP, Sho1p-GFP, and Opy2p-GFP strains with or without *pGAL-ALY1*. Cells were grown in YEP-GAL media. (E) Localization of pMsb2p-GFP in a *GAL-ALY1* strain. Bar, 5 μm.

ing defect seen in the *snf8Δ* mutant is due to a defect in the Rim101 pathway and not the ESCRT pathway.

**Analysis of Msb2p function in trafficking mutants is consistent with its MAPK function at the PM.** Previous results indicated that Msb2p signals from the PM (29). To test whether Msb2p is delivered to the PM for its subsequent delivery to the vacuole, a mutant defective in PM delivery of proteins was examined. Immunoblot analysis of Msb2<sup>p</sup> in the *sec3-2* mutant, which is defective for exocytosis (93), showed stabilization of the protein to the same levels as seen in the *pep4Δ* mutant (Fig. 6A). This result indicates that Msb2p must be delivered to the PM in order to be internalized and turned over in the vacuole.

We also found that cells overproducing *ALY1*, a member of the arrestin-related trafficking adaptor (ART) family of protein trafficking adaptors (94), showed mislocalization of Msb2p that corresponded to reduced activity of the filamentous growth pathway. *ALY1* was identified in a genetic screen for genes that when over-

expressed dampened the *FUS1-HIS3* growth reporter in cells lacking an intact mating pathway (*ste4Δ*). *ALY1* was identified, along with *RCK2*, which regulates the HOG pathway (95, 96) and which has been described in terms of its role in regulating the filamentous growth pathway (47). Cells overproducing *ALY1* showed mislocalization of Msb2p to the vacuolar membrane (Fig. 6E). The localization of Msb2p to the PM requires PI (4)P (70). Overexpression of *ALY1* did not impact the localization of a PI(4,5)P<sub>2</sub> PM marker (pFLARE, fluorescent lipid-associated reporter, PH domain of PLC-δ; see Fig. S5 in the supplemental material). As a result, Msb2p (and Opy2p) were stabilized, because they were not delivered to the vacuolar lumen (Fig. 6D and see Fig. S5 in the supplemental material). In these cells, the filamentous growth pathway was attenuated (Fig. 6B), and cells failed to undergo invasive growth (Fig. 6C). These results support the idea that Msb2p is delivered to the PM to activate the MAPK pathway. This conclusion is consistent with the idea that a version of Msb2p that

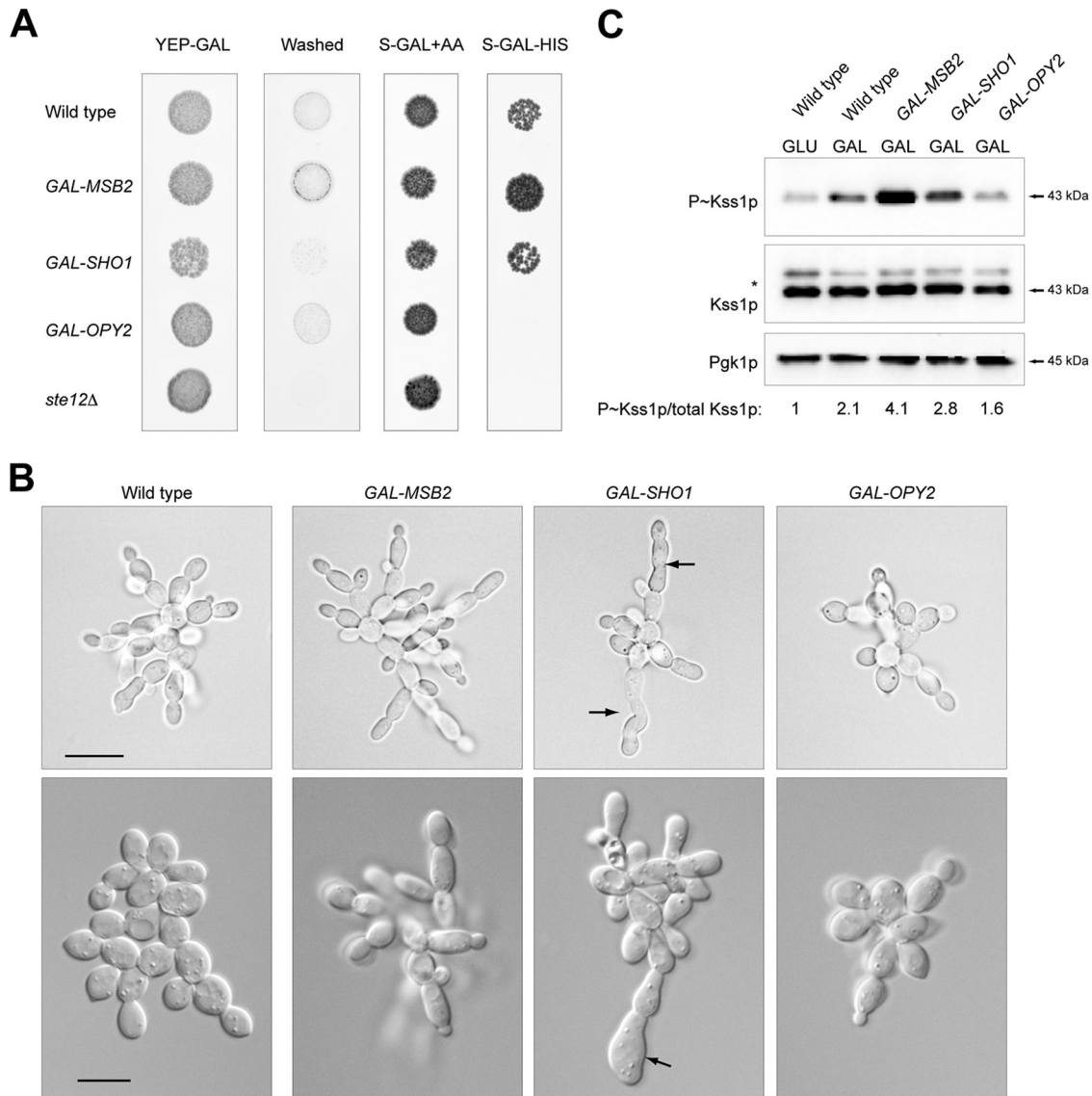


**FIG 7** Differences in the filamentous growth output by the three PM proteins. (A) Plate washing assay and *ste4 FUS1-HIS3* reporter assay for strains are shown. Equal amounts of cells were spotted. (B) Single-cell invasive growth assay of the indicated strains. Upper panel, microscopic images of the indicated strains in YEP-GAL; lower panel, single-cell invasive growth assay of the indicated strains. Representative cells are shown. Bar, 5  $\mu$ m. (C) Phosphorylated Kss1p levels in the indicated strains grown in YEP-GAL media.

cannot be internalized from the PM shows elevated MAPK activity (29). Accordingly, mistargeting of Msb2p to the vacuolar membrane results in reduced MAPK activity.

We also tested whether the Msb2p, Sho1p, or Opy2p showed altered signaling in retromer mutants. Retromer is a trimeric complex (Vps26p, Vps29p, and Vps36p) that recycles certain PM proteins to the Golgi compartment, from where they can be trafficked back to the PM (97, 98). In the *vps26Δ* mutant, MAPK activity was not impacted based on P~Kss1p levels (see Fig. S6A in the supplemental material), and the *ste4 FUS1-HIS3* reporter (see Fig. S6B in the supplemental material). The localization of the proteins was normal (see Fig. S6C in the supplemental material). However, the *vps26Δ* and *vps35Δ* mutants did show a reduction in filamentous growth by the single cell assay (see Fig. S6D in the supplemental material), and a minor

reduction in invasive growth by the plate-washing assay (see Fig. S6B in the supplemental material), which may indicate a minor role for the proteins in regulating the MAPK pathway or a role for the proteins in regulating filamentous growth outside the MAPK pathway, since many proteins and pathways regulate the response (99).

**Functional differences between TM regulators were identified by genetic analysis.** We also tested whether Msb2p, Sho1p, and Opy2p have different functions in regulating aspects of the filamentation response. Overexpression of *MSB2* was previously shown to cause hyper-invasive growth (30, 91). This turned out to be an *MSB2*-specific phenotype, as overexpression of *SHO1* and *OPY2* did not induce hyperinvasive growth (Fig. 7A). Overexpression of *SHO1* induces hyperpolarized growth (28). This was a *SHO1*-specific phenotype, since overexpression of *MSB2* or *OPY2*

did not cause hyperpolarized growth (Fig. 7B, arrows). Overexpression of *OPY2* dampens the mating pathway reporter *FUS1* (35, 38). This was an *Opy2p*-specific phenotype because overexpression of *MSB2* or *SHO1* did not attenuate *FUS1-HIS3* expression (Fig. 7A, right panels). The filamentous growth pathway activity was measured in cells overexpressing the three TM proteins. Overexpression of *Msb2p* induced phosphorylation of *Kss1p*, whereas overexpression of *SHO1* had relatively little effect (Fig. 7C). Overexpression of *Opy2p* caused a decrease in *P~Kss1p* levels, suggesting that *Opy2p* might have a yet unexplored role in attenuating the filamentous growth pathway (Fig. 7C). Based on these tests, *Msb2p*, *Sho1p*, and *Opy2p* may have pathway-specific roles in regulating filamentous growth.

## DISCUSSION

Many signaling pathways are regulated by multiple TM proteins that work together in some manner to produce a downstream signal. Here, we investigated the functional roles of TM proteins that regulate the filamentous growth pathway. We show that *Msb2p*, *Sho1p*, and *Opy2p* associate by co-IP analysis. This interaction may facilitate the interaction between cytosolic regulators of the filamentous growth pathway. *Msb2p* associates with versions of *Cdc42p* that mimic the GTP-bound (active) conformation of the GTPase (30). *Cdc42p* is also anchored to the PM by the lipid modification geranylgeranylation (100, 101). *Sho1p* associates with the MAPKKK *Ste11p* and the adaptor *Ste50p*. This has been explicitly shown for the HOG pathway (44, 102, 103) and likely occurs in the filamentous growth pathway as well. *Opy2p* also interacts with *Ste50p* (33, 36, 37, 104). Thus, the association between *Msb2p*, *Sho1p*, and *Opy2p* may facilitate interactions between *Cdc42p*-PAK and its substrate for the filamentation pathway, the MAPKKK *Ste11p*.

Perhaps unexpectedly, the TM regulators have different localization patterns. The different localization patterns can be explained in two ways. First, each protein has a unique pattern. For example, *Sho1p* is typically found in large cells at the mother-bud neck, whereas *Msb2p* or *Opy2p* are not. Second, the proteins have different rates of turnover from the PM (Fig. 8). *Msb2p* is turned over rapidly from the PM, which attenuates the filamentous growth pathway. *Opy2p* is turned over at an intermediate rate, whereas *Sho1p* is turned over at a low rate. In general, the turnover of yeast proteins from the PM requires the ubiquitin ligase *Rsp5p* (105). Different adaptors, or (arrestin) ARTs, regulate the turnover of different PM proteins (94). Possibly, different ART combinations may regulate the differential turnover of TM proteins that regulate the filamentous growth pathway.

The fact that *Msb2p*, *Sho1p*, and *Opy2p* do not predominantly colocalize at the PM indicates that transient interactions may be sufficient for MAPK signaling. One possibility is that *Sho1p* forms a stable cortical mark at the PM to which *Msb2p* and *Opy2p* transiently associate. Given that *Msb2p*, *Sho1p*, and *Opy2p* have been implicated in HOG pathway signaling and therefore respond to a variety of stimuli, it will be interesting to determine whether different trafficking/turnover mechanisms for the proteins lead to pathway-specific outputs. *Msb2p*, *Sho1p*, and *Opy2p* proteins have orthologs in other fungal species, including filamentous fungi that can be pathogenic (106–111). Thus, the regulatory mechanisms described here may apply to these PM sensors in other fungal species.

The filamentous growth pathway is similar in some respects to

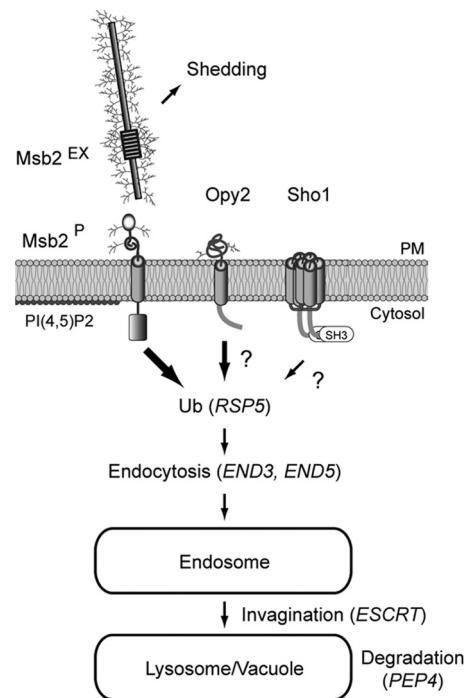


**FIG 8** Model for turnover of PM sensors of the filamentous growth pathway. In the model, *Msb2p*, *Sho1p*, and *Opy2p* are delivered to the PM by exocytosis. *Msb2p* is processed into a shed extracellular domain (*Msb2<sup>EX</sup>*) and a cell-associated signaling domain (*Msb2<sup>P</sup>*). The proteins regulate the filamentous growth pathway at the PM. *Msb2<sup>P</sup>* is rapidly turned over in an *Rsp5p*-dependent manner to attenuate the filamentous growth pathway (big arrow). *Opy2p* is turned over at an intermediate rate (medium arrow), and *Sho1p* is turned over at a low rate (small arrow). How the turnover of *Opy2p* and *Sho1p* is regulated is not clear (question marks). After endocytosis from the PM, *Msb2p* and *Opy2p* proteins are trafficked to the vacuole in an ESCRT-dependent manner. How *Sho1p* is delivered to the vacuole is not clear. Ub, ubiquitin.

the PKC pathway. Multiple TM proteins regulate the PKC pathway, including *Wsc1p*/*Sgl1p*, *Wsc2p*, *Wsc3p*, and *Mid2p* (112). *Wsc1p* is a single transmembrane domain cell wall sensor that when marked with GFP does not yield a heavy vacuolar signal (72). The *Wsc1p* protein localizes to the PM dependent on the ESCRT pathway recycling it (72). This recycling is dependent on *Sla1p*. In comparison, neither *Msb2p* nor *Opy1p* require *Sla1p*, and these proteins do not have NPFXD endocytosis signals similar to those of *Wsc1p*. Thus, one can envision a possibility where each TM regulator possess its own localization pattern and mode of turnover. Dissecting regulatory features of differential turnover of TM proteins will be important to understand the overall regulation of signaling pathways.

Many proteins accumulate in the MVB in ESCRT mutants. These include *Notch* (73), *Smoothed*, the receptor for *Hedgehog* (113), *epidermal growth factor receptor* (114, 115), and *CXCR4* (115). Few proteins accumulate at the cell cortex in ESCRT mutants (116, 117). It is noteworthy that *Msb2p* accumulates at the MVB in ESCRT mutants, whereas *Sho1p* accumulates at the PM. This might be explained, in part, because *Sho1p* is in an inactive state. When activated, the localization of *Sho1p* is more dynamic, and the protein can be found in internal compartments. Some receptors can signal from endosomes after they have been turned over from the PM. *Epidermal growth factor receptor* can

signal from endosomes, in early ESCRT mutants (114). In *Drosophila* mutants lacking the ESCRT component Vps25p, Notch accumulates in the endosome and induces signaling from that site (118). Intracellular G-protein coupled receptor (GPCR) signaling has been documented in several studies that show internalized GPCRs sustain MAPK signaling (119). We show, by disentangling regulation by the RIM101 and ESCRT pathways, that Msb2p does not show enhanced signaling from endosomes. Thus, Msb2p signaling is attenuated by a mechanism that requires other factors than the ESCRT pathway.

## ACKNOWLEDGMENTS

We thank Nadia Vadaie, Umami Abdullah, and Trinity Bernier-Natchway for help with experiments. We thank Scott Emr, John Pringle, Charlie Boone, Alan Davidson, and Hiten Madhani for reagents.

P.J.C. is supported by a grant from the U.S. Public Health Service (GM098629).

## REFERENCES

- Wendland J. 2001. Comparison of morphogenetic networks of filamentous fungi and yeast. *Fungal Genet Biol* 34:63–82. <http://dx.doi.org/10.1006/fgbi.2001.1290>.
- Whiteway M, Bachewich C. 2007. Morphogenesis in *Candida albicans*. *Annu Rev Microbiol* 61:529–553. <http://dx.doi.org/10.1146/annurev.micro.61.080706.093341>.
- Lo HJ, Kohler JR, DiDomenico B, Loebenberg D, Cacciapuoti A, Fink GR. 1997. Nonfilamentous *C. albicans* mutants are avirulent. *Cell* 90:939–949. [http://dx.doi.org/10.1016/S0092-8674\(00\)80358-X](http://dx.doi.org/10.1016/S0092-8674(00)80358-X).
- Lengeler KB, Davidson RC, D'Souza C, Harashima T, Shen WC, Wang P, Pan X, Waugh M, Heitman J. 2000. Signal transduction cascades regulating fungal development and virulence. *Microbiol Mol Biol Rev* 64:746–785. <http://dx.doi.org/10.1128/MMBR.64.4.746-785.2000>.
- Dalle F, Wachtler B, L'Ollivier C, Holland G, Bannert N, Wilson D, Labruere C, Bonnin A, Hube B. 2010. Cellular interactions of *Candida albicans* with human oral epithelial cells and enterocytes. *Cell Microbiol* 12:248–271. <http://dx.doi.org/10.1111/j.1462-5822.2009.01394.x>.
- Gimeno CJ, Ljungdahl PO, Styles CA, Fink GR. 1992. Unipolar cell divisions in the yeast *Saccharomyces cerevisiae* lead to filamentous growth: regulation by starvation and RAS. *Cell* 68:1077–1090. [http://dx.doi.org/10.1016/0092-8674\(92\)90079-R](http://dx.doi.org/10.1016/0092-8674(92)90079-R).
- Verstrepen KJ, Klis FM. 2006. Flocculation, adhesion and biofilm formation in yeasts. *Mol Microbiol* 60:5–15. <http://dx.doi.org/10.1111/j.1365-2958.2006.05072.x>.
- Kron SJ, Styles CA, Fink GR. 1994. Symmetric cell division in pseudohyphae of the yeast *Saccharomyces cerevisiae*. *Mol Biol Cell* 5:1003–1022. <http://dx.doi.org/10.1091/mbc.5.9.1003>.
- Rua D, Tobe BT, Kron SJ. 2001. Cell cycle control of yeast filamentous growth. *Curr Opin Microbiol* 4:720–727. [http://dx.doi.org/10.1016/S1369-5274\(01\)00274-0](http://dx.doi.org/10.1016/S1369-5274(01)00274-0).
- Borneman AR, Leigh-Bell JA, Yu H, Bertone P, Gerstein M, Snyder M. 2006. Target hub proteins serve as master regulators of development in yeast. *Genes Dev* 20:435–448. <http://dx.doi.org/10.1101/gad.1389306>.
- Mosch HU, Kubler E, Krappmann S, Fink GR, Braus GH. 1999. Crosstalk between the Ras2p-controlled mitogen-activated protein kinase and cAMP pathways during invasive growth of *Saccharomyces cerevisiae*. *Mol Biol Cell* 10:1325–1335. <http://dx.doi.org/10.1091/mbc.10.5.1325>.
- Mosch HU, Roberts RL, Fink GR. 1996. Ras2 signals via the Cdc42/Ste20/mitogen-activated protein kinase module to induce filamentous growth in *Saccharomyces cerevisiae*. *Proc Natl Acad Sci U S A* 93:5352–5356. <http://dx.doi.org/10.1073/pnas.93.11.5352>.
- Rohde JR, Cardenas ME. 2004. Nutrient signaling through TOR kinases controls gene expression and cellular differentiation in fungi. *Curr Top Microbiol Immunol* 279:53–72.
- Roberts RL, Fink GR. 1994. Elements of a single MAP kinase cascade in *Saccharomyces cerevisiae* mediate two developmental programs in the same cell type: mating and invasive growth. *Genes Dev* 8:2974–2985. <http://dx.doi.org/10.1101/gad.8.24.2974>.
- Borneman AR, Gianoulis TA, Zhang ZD, Yu H, Rozowsky J, Seringhaus MR, Wang LY, Gerstein M, Snyder M. 2007. Divergence of transcription factor binding sites across related yeast species. *Science* 317:815–819. <http://dx.doi.org/10.1126/science.1140748>.
- Johnson DI. 1999. Cdc42: an essential Rho-type GTPase controlling eukaryotic cell polarity. *Microbiol Mol Biol Rev* 63:54–105.
- Bi E, Park HO. 2012. Cell polarization and cytokinesis in budding yeast. *Genetics* 191:347–387. <http://dx.doi.org/10.1534/genetics.111.132886>.
- Leberer E, Wu C, Leeuw T, Fourest-Lieuvin A, Segall JE, Thomas DY. 1997. Functional characterization of the Cdc42p binding domain of yeast Ste20p protein kinase. *EMBO J* 16:83–97. <http://dx.doi.org/10.1093/emboj/16.1.83>.
- Peter M, Neiman AM, Park HO, van Lohuizen M, Herskowitz I. 1996. Functional analysis of the interaction between the small GTP binding protein Cdc42 and the Ste20 protein kinase in yeast. *EMBO J* 15:7046–7059.
- Pitoniak A, Chavel CA, Chow J, Smith J, Camara D, Karunanithi S, Li B, Wolfe KH, Cullen PJ. 2015. Cdc42p-interacting protein bem4p regulates the filamentous-growth mitogen-activated protein kinase pathway. *Mol Cell Biol* 35:417–436. <http://dx.doi.org/10.1128/MCB.00850-14>.
- Madhani HD, Styles CA, Fink GR. 1997. MAP kinases with distinct inhibitory functions impart signaling specificity during yeast differentiation. *Cell* 91:673–684. [http://dx.doi.org/10.1016/S0092-8674\(00\)80454-7](http://dx.doi.org/10.1016/S0092-8674(00)80454-7).
- Madhani HD, Fink GR. 1997. Combinatorial control required for the specificity of yeast MAPK signaling. *Science* 275:1314–1317. <http://dx.doi.org/10.1126/science.275.5304.1314>.
- van der Felden J, Weisser S, Bruckner S, Lenz P, Mosch HU. 2014. The transcription factors Tec1 and Ste12 interact with coregulators Msa1 and Msa2 to activate adhesion and multicellular development. *Mol Cell Biol* 34:2283–2293. <http://dx.doi.org/10.1128/MCB.01599-13>.
- Rupp S, Summers E, Lo HJ, Madhani H, Fink G. 1999. MAP kinase and cAMP filamentation signaling pathways converge on the unusually large promoter of the yeast FLO11 gene. *EMBO J* 18:1257–1269. <http://dx.doi.org/10.1093/emboj/18.5.1257>.
- Roberts CJ, Nelson B, Marton MJ, Stoughton R, Meyer MR, Bennett HA, He YD, Dai H, Walker WL, Hughes TR, Tyers M, Boone C, Friend SH. 2000. Signaling and circuitry of multiple MAPK pathways revealed by a matrix of global gene expression profiles. *Science* 287:873–880. <http://dx.doi.org/10.1126/science.287.5454.873>.
- Carraway KL, Ramsauer VP, Haq B, Carothers Carraway CA. 2003. Cell signaling through membrane mucins. *Bioessays* 25:66–71. <http://dx.doi.org/10.1002/bies.10201>.
- Singh PK, Hollingsworth MA. 2006. Cell surface-associated mucins in signal transduction. *Trends Cell Biol* 16:467–476. <http://dx.doi.org/10.1016/j.tcb.2006.07.006>.
- Vadaie N, Dionne H, Akajagbor DS, Nickerson SR, Krysan DJ, Cullen PJ. 2008. Cleavage of the signaling mucin Msb2 by the aspartyl protease Yps1 is required for MAPK activation in yeast. *J Cell Biol* 181:1073–1081. <http://dx.doi.org/10.1083/jcb.200704079>.
- Adhikari H, Vadaie N, Chow J, Cammisse LM, Chavel CA, Li B, Bowitch A, Stefan CJ, Cullen PJ. 2015. Role of the unfolded protein response in regulating the mucin-dependent filamentous growth MAPK pathway. *Mol Cell Biol* 35:1414–1432. <http://dx.doi.org/10.1128/MCB.01501-14>.
- Cullen PJ, Sabbagh W, Jr, Graham E, Irick MM, van Olden EK, Neal C, Delrow J, Bardwell L, Sprague GF, Jr. 2004. A signaling mucin at the head of the Cdc42- and MAPK-dependent filamentous growth pathway in yeast. *Genes Dev* 18:1695–1708. <http://dx.doi.org/10.1101/gad.1178604>.
- O'Rourke SM, Herskowitz I. 1998. The Hog1 MAPK prevents cross talk between the HOG and pheromone response MAPK pathways in *Saccharomyces cerevisiae*. *Genes Dev* 12:2874–2886. <http://dx.doi.org/10.1101/gad.12.18.2874>.
- Shimada Y, Wiget P, Gulli MP, Bi E, Peter M. 2004. The nucleotide exchange factor Cdc24p may be regulated by auto-inhibition. *EMBO J* 23:1051–1062. <http://dx.doi.org/10.1038/sj.emboj.7600124>.
- Yamamoto K, Tatebayashi K, Tanaka K, Saito H. 2010. Dynamic control of yeast MAP kinase network by induced association and dissociation between the Ste50 scaffold and the Opy2 membrane anchor. *Mol Cell* 40:87–98. <http://dx.doi.org/10.1016/j.molcel.2010.09.011>.
- Yang HY, Tatebayashi K, Yamamoto K, Saito H. 2009. Glycosylation defects activate filamentous growth Kss1 MAPK and inhibit osmoregu-

- latory Hog1 MAPK. *EMBO J* 28:1380–1391. <http://dx.doi.org/10.1038/emboj.2009.104>.
35. Karunanithi S, Cullen PJ. 2012. The filamentous growth MAPK pathway responds to glucose starvation through the Mig1/2 transcriptional repressors in *Saccharomyces cerevisiae*. *Genetics* 192:869–887. <http://dx.doi.org/10.1534/genetics.112.142661>.
  36. Ekiel I, Sulea T, Jansen G, Kowalik M, Minailiuc O, Cheng J, Harcus D, Cygler M, Whiteway M, Wu C. 2009. Binding the atypical RA domain of Ste50p to the unfolded Opy2p cytoplasmic tail is essential for the high-osmolarity glycerol pathway. *Mol Biol Cell* 20:5117–5126. <http://dx.doi.org/10.1091/mbc.E09-07-0645>.
  37. Wu C, Jansen G, Zhang J, Thomas DY, Whiteway M. 2006. Adaptor protein Ste50p links the Ste11p MEKK to the HOG pathway through plasma membrane association. *Genes Dev* 20:734–746. <http://dx.doi.org/10.1101/gad.1375706>.
  38. Cappell SD, Dohlman HG. 2011. Selective regulation of MAP kinase signaling by an endomembrane phosphatidylinositol 4-kinase. *J Biol Chem* 286:14852–14860. <http://dx.doi.org/10.1074/jbc.M110.195073>.
  39. Tatebayashi K, Tanaka K, Yang HY, Yamamoto K, Matsushita Y, Tomida T, Imai M, Saito H. 2007. Transmembrane mucins Hkr1 and Msb2 are putative osmosensors in the SHO1 branch of yeast HOG pathway. *EMBO J* 26:3521–3533. <http://dx.doi.org/10.1038/sj.emboj.7601796>.
  40. O'Rourke SM, Herskowitz I. 2002. A third osmosensing branch in *Saccharomyces cerevisiae* requires the Msb2 protein and functions in parallel with the Sho1 branch. *Mol Cell Biol* 22:4739–4749. <http://dx.doi.org/10.1128/MCB.22.13.4739-4749.2002>.
  41. Raitt DC, Posas F, Saito H. 2000. Yeast Cdc42 GTPase and Ste20 PAK-like kinase regulate Sho1-dependent activation of the Hog1 MAPK pathway. *EMBO J* 19:4623–4631. <http://dx.doi.org/10.1093/emboj/19.17.4623>.
  42. Reiser V, Salah SM, Ammerer G. 2000. Polarized localization of yeast Pbs2 depends on osmolarity, the membrane protein Sho1 and Cdc42. *Nat Cell Biol* 2:620–627. <http://dx.doi.org/10.1038/35023568>.
  43. Maeda T, Takekawa M, Saito H. 1995. Activation of yeast PBS2 MAPKK by MAPKKs or by binding of an SH3-containing osmosensor. *Science* 269:554–558. <http://dx.doi.org/10.1126/science.7624781>.
  44. Tatebayashi K, Yamamoto K, Nagoya M, Takayama T, Nishimura A, Sakurai M, Momma T, Saito H. 2015. Osmosensing and scaffolding functions of the oligomeric four-transmembrane domain osmosensor Sho1. *Nat Commun* 6:6975. <http://dx.doi.org/10.1038/ncomms7975>.
  45. Hohmann S, Krantz M, Nordlander B. 2007. Yeast osmoregulation. *Methods Enzymol* 428:29–45. [http://dx.doi.org/10.1016/S0076-6879\(07\)28002-4](http://dx.doi.org/10.1016/S0076-6879(07)28002-4).
  46. Saito H. 2010. Regulation of cross-talk in yeast MAPK signaling pathways. *Curr Opin Microbiol* 13:677–683. <http://dx.doi.org/10.1016/j.mib.2010.09.001>.
  47. Pitoniak A, Birkaya B, Dionne HM, Vadaie N, Cullen PJ. 2009. The signaling mucins Msb2 and Hkr1 differentially regulate the filamentation mitogen-activated protein kinase pathway and contribute to a multimodal response. *Mol Biol Cell* 20:3101–3114. <http://dx.doi.org/10.1091/mbc.E08-07-0760>.
  48. Hao N, Behar M, Parnell SC, Torres MP, Borchers CH, Elston TC, Dohlman HG. 2007. A systems-biology analysis of feedback inhibition in the Sho1 osmotic-stress-response pathway. *Curr Biol* 17:659–667. <http://dx.doi.org/10.1016/j.cub.2007.02.044>.
  49. Levin DE. 2005. Cell wall integrity signaling in *Saccharomyces cerevisiae*. *Microbiol Mol Biol Rev* 69:262–291. <http://dx.doi.org/10.1128/MMBR.69.2.262-291.2005>.
  50. Rodicio R, Heinisch JJ. 2010. Together we are strong—cell wall integrity sensors in yeasts. *Yeast* 27:531–540. <http://dx.doi.org/10.1002/yea.1785>.
  51. Yarden Y. 2001. The EGFR family and its ligands in human cancer: signaling mechanisms and therapeutic opportunities. *Eur J Cancer* 37(Suppl 4):S3–S8. [http://dx.doi.org/10.1016/S0959-8049\(01\)80495-0](http://dx.doi.org/10.1016/S0959-8049(01)80495-0).
  52. Doroquez DB, Rebay I. 2006. Signal integration during development: mechanisms of EGFR and Notch pathway function and cross-talk. *Crit Rev Biochem Mol Biol* 41:339–385. <http://dx.doi.org/10.1080/10409230600914344>.
  53. Sambrook J, Fritsch EF, Maniatis T. 1989. *Molecular cloning: a laboratory manual*. Cold Spring Harbor Laboratory Press, Cold Spring Harbor, NY.
  54. Rose MD, Winston F, Hieter P. 1990. *Methods in yeast genetics*. Cold Spring Harbor Laboratory Press, Cold Spring Harbor, NY.
  55. McCaffrey G, Clay FJ, Kelsay K, Sprague GF, Jr. 1987. Identification and regulation of a gene required for cell fusion during mating of the yeast *Saccharomyces cerevisiae*. *Mol Cell Biol* 7:2680–2690.
  56. Cullen PJ, Sprague GF, Jr. 2000. Glucose depletion causes haploid invasive growth in yeast. *Proc Natl Acad Sci U S A* 97:13619–13624. <http://dx.doi.org/10.1073/pnas.240345197>.
  57. Gelperin DM, White MA, Wilkinson ML, Kon Y, Kung LA, Wise KJ, Lopez-Hoyo N, Jiang L, Piccirillo S, Yu H, Gerstein M, Dumont ME, Phizicky EM, Snyder M, Grayhack EJ. 2005. Biochemical and genetic analysis of the yeast proteome with a movable ORF collection. *Genes Dev* 19:2816–2826. <http://dx.doi.org/10.1101/gad.1362105>.
  58. Baudin A, Ozier-Kalogeropoulos O, Denouel A, Lacroute F, Cullin C. 1993. A simple and efficient method for direct gene deletion in *Saccharomyces cerevisiae*. *Nucleic Acids Res* 21:3329–3330. <http://dx.doi.org/10.1093/nar/21.14.3329>.
  59. Longtine MS, McKenzie A, III, Demarini DJ, Shah NG, Wach A, Brachet A, Philippsen P, Pringle JR. 1998. Additional modules for versatile and economical PCR-based gene deletion and modification in *Saccharomyces cerevisiae*. *Yeast* 14:953–961. [http://dx.doi.org/10.1002/\(SICI\)1097-0061\(199807\)14:10<953::AID-YEA293>3.3.CO;2-L](http://dx.doi.org/10.1002/(SICI)1097-0061(199807)14:10<953::AID-YEA293>3.3.CO;2-L).
  60. Goldstein AL, McCusker JH. 1999. Three new dominant drug resistance cassettes for gene disruption in *Saccharomyces cerevisiae*. *Yeast* 15:1541–1553. [http://dx.doi.org/10.1002/\(SICI\)1097-0061\(199910\)15:14<1541::AID-YEA476>3.0.CO;2-K](http://dx.doi.org/10.1002/(SICI)1097-0061(199910)15:14<1541::AID-YEA476>3.0.CO;2-K).
  61. Schneider BL, Seufert W, Steiner B, Yang QH, Futcher AB. 1995. Use of polymerase chain reaction epitope tagging for protein tagging in *Saccharomyces cerevisiae*. *Yeast* 11:1265–1274. <http://dx.doi.org/10.1002/yea.320111306>.
  62. Marles JA, Dahesh S, Haynes J, Andrews BJ, Davidson AR. 2004. Protein-protein interaction affinity plays a crucial role in controlling the Sho1p-mediated signal transduction pathway in yeast. *Mol Cell* 14:813–823. <http://dx.doi.org/10.1016/j.molcel.2004.05.024>.
  63. Stefan CJ, Audhya A, Emr SD. 2002. The yeast synaptojanin-like proteins control the cellular distribution of phosphatidylinositol (4,5)-bisphosphate. *Mol Biol Cell* 13:542–557. <http://dx.doi.org/10.1091/mbc.01-10-0476>.
  64. Ramer SW, Elledge SJ, Davis RW. 1992. Dominant genetics using a yeast genomic library under the control of a strong inducible promoter. *Proc Natl Acad Sci U S A* 89:11589–11593. <http://dx.doi.org/10.1073/pnas.89.23.11589>.
  65. Wach A, Brachet A, Alberti-Segui C, Rebischung C, Philippsen P. 1997. Heterologous HIS3 marker and GFP reporter modules for PCR-targeting in *Saccharomyces cerevisiae*. *Yeast* 13:1065–1075. [http://dx.doi.org/10.1002/\(SICI\)1097-0061\(199709\)13:11<1065::AID-YEA159>3.0.CO;2-K](http://dx.doi.org/10.1002/(SICI)1097-0061(199709)13:11<1065::AID-YEA159>3.0.CO;2-K).
  66. Conibear E, Stevens TH. 2002. Studying yeast vacuoles. *Methods Enzymol* 351:408–432. [http://dx.doi.org/10.1016/S0076-6879\(02\)51861-9](http://dx.doi.org/10.1016/S0076-6879(02)51861-9).
  67. Adhikari H, Cullen PJ. 2014. Metabolic respiration induces AMPK- and Ire1p-dependent activation of the p38-type HOG MAPK pathway. *PLoS Genet* 10:e1004734. <http://dx.doi.org/10.1371/journal.pgen.1004734>.
  68. Kemp HA, Sprague GF, Jr. 2003. Far3 and five interacting proteins prevent premature recovery from pheromone arrest in the budding yeast *Saccharomyces cerevisiae*. *Mol Cell Biol* 23:1750–1763. <http://dx.doi.org/10.1128/MCB.23.5.1750-1763.2003>.
  69. Karunanithi S, Cullen PJ. 2012. The filamentous growth MAPK pathway responds to glucose starvation through the Mig1/2 transcriptional repressors in *Saccharomyces cerevisiae*. *Genetics* 192:869–887. <http://dx.doi.org/10.1534/genetics.112.142661>.
  70. Adhikari H, Cullen PJ. 2015. Role of phosphatidylinositol phosphate signaling in the regulation of the filamentous growth MAPK pathway. *Eukaryot Cell* 14:427–440. <http://dx.doi.org/10.1128/EC.00013-15>.
  71. Obrig TG, Culp WJ, McKeenan WL, Hardesty B. 1971. The mechanism by which cycloheximide and related glutarimide antibiotics inhibit peptide synthesis on reticulocyte ribosomes. *J Biol Chem* 246:174–181.
  72. Piao HL, Machado IM, Payne GS. 2007. NPFXD-mediated endocytosis is required for polarity and function of a yeast cell wall stress sensor. *Mol Biol Cell* 18:57–65.
  73. Wegner CS, Rodahl LM, Stenmark H. 2011. ESCRT proteins and cell signaling. *Traffic* 12:1291–1297. <http://dx.doi.org/10.1111/j.1600-0854.2011.01210.x>.
  74. MacGurn JA, Hsu PC, Emr SD. 2012. Ubiquitin and membrane protein turnover: from cradle to grave. *Annu Rev Biochem* 81:231–259. <http://dx.doi.org/10.1146/annurev-biochem-060210-093619>.

75. Zhao Y, Macgurn JA, Liu M, Emr S. 2013. The ART-Rsp5 ubiquitin ligase network comprises a plasma membrane quality control system that protects yeast cells from proteotoxic stress. *eLife* 2:e00459. <http://dx.doi.org/10.7554/eLife.00459>.
76. Ammerer G, Hunter CP, Rothman JH, Saari GC, Valls LA, Stevens TH. 1986. PEP4 gene of *Saccharomyces cerevisiae* encodes proteinase A, a vacuolar enzyme required for processing of vacuolar precursors. *Mol Cell Biol* 6:2490–2499.
77. Hurley JH, Emr SD. 2006. The ESCRT complexes: structure and mechanism of a membrane-trafficking network. *Annu Rev Biophys Biomol Struct* 35:277–298. <http://dx.doi.org/10.1146/annurev.biophys.35.040405.102126>.
78. Teis D, Saksena S, Emr SD. 2009. SnapShot: the ESCRT machinery. *Cell* 137:182–182 e181. <http://dx.doi.org/10.1016/j.cell.2009.03.027>.
79. Russell MR, Nickerson DP, Odorizzi G. 2006. Molecular mechanisms of late endosome morphology, identity and sorting. *Curr Opin Cell Biol* 18:422–428. <http://dx.doi.org/10.1016/j.ccb.2006.06.002>.
80. Saksena S, Sun J, Chu T, Emr SD. 2007. ESCRTing proteins in the endocytic pathway. *Trends Biochem Sci* 32:561–573. <http://dx.doi.org/10.1016/j.tibs.2007.09.010>.
81. Vida TA, Emr SD. 1995. A new vital stain for visualizing vacuolar membrane dynamics and endocytosis in yeast. *J Cell Biol* 128:779–792. <http://dx.doi.org/10.1083/jcb.128.5.779>.
82. Stefan CJ, Blumer KJ. 1994. The third cytoplasmic loop of a yeast G-protein-coupled receptor controls pathway activation, ligand discrimination, and receptor internalization. *Mol Cell Biol* 14:3339–3349.
83. Haugh JM, Meyer T. 2002. Active EGF receptors have limited access to PtdIns(4,5)P(2) in endosomes: implications for phospholipase C and PI 3-kinase signaling. *J Cell Sci* 115:303–310.
84. Joo EJ, Chun J, Ha YW, Ko HJ, Xu MY, Kim YS. 2015. Novel roles of ginsenoside Rg3 in apoptosis through downregulation of epidermal growth factor receptor. *Chem-Biol Interact* 233:25–34. <http://dx.doi.org/10.1016/j.cbi.2015.03.016>.
85. Joazeiro CA, Wing SS, Huang H, Levenson JD, Hunter T, Liu YC. 1999. The tyrosine kinase negative regulator c-Cbl as a RING-type, E2-dependent ubiquitin-protein ligase. *Science* 286:309–312. <http://dx.doi.org/10.1126/science.286.5438.309>.
86. Levkowitz G, Waterman H, Ettenberg SA, Katz M, Tsygankov AY, Alroy I, Lavi S, Iwai K, Reiss Y, Ciechanover A, Lipkowitz S, Yarden Y. 1999. Ubiquitin ligase activity and tyrosine phosphorylation underlie suppression of growth factor signaling by c-Cbl/Sli-1. *Mol Cell* 4:1029–1040. [http://dx.doi.org/10.1016/S1097-2765\(00\)80231-2](http://dx.doi.org/10.1016/S1097-2765(00)80231-2).
87. Lee MJ, Dohlman HG. 2008. Coactivation of G protein signaling by cell-surface receptors and an intracellular exchange factor. *Curr Biol* 18:211–215. <http://dx.doi.org/10.1016/j.cub.2008.01.007>.
88. Chavel CA, Dionne HM, Birkaya B, Joshi J, Cullen PJ. 2010. Multiple signals converge on a differentiation MAPK pathway. *PLoS Genet* 6:e1000883. <http://dx.doi.org/10.1371/journal.pgen.1000883>.
89. Sarode N, Miracle B, Peng X, Ryan O, Reynolds TB. 2011. Vacuolar protein sorting genes regulate mat formation in *Saccharomyces cerevisiae* by Flo11p-dependent and -independent mechanisms. *Eukaryot Cell* 10:1516–1526. <http://dx.doi.org/10.1128/EC.05078-11>.
90. Cornet M, Bidard F, Schwarz P, Da Costa G, Blanchin-Roland S, Dromer F, Gaillardin C. 2005. Deletions of endocytic components VPS28 and VPS32 affect growth at alkaline pH and virulence through both RIM101-dependent and RIM101-independent pathways in *Candida albicans*. *Infect Immun* 73:7977–7987. <http://dx.doi.org/10.1128/IAI.73.12.7977-7987.2005>.
91. Chavel CA, Caccamise LM, Li B, Cullen PJ. 2014. Global regulation of a differentiation MAPK pathway in yeast. *Genetics* 198:1309–1328. <http://dx.doi.org/10.1534/genetics.114.168252>.
92. Li W, Mitchell AP. 1997. Proteolytic activation of Rim1p, a positive regulator of yeast sporulation and invasive growth. *Genetics* 145:63–73.
93. Finger FP, Novick P. 1997. Sec3p is involved in secretion and morphogenesis in *Saccharomyces cerevisiae*. *Mol Biol Cell* 8:647–662. <http://dx.doi.org/10.1091/mbc.8.4.647>.
94. Lin CH, MacGurn JA, Chu T, Stefan CJ, Emr SD. 2008. Arrestin-related ubiquitin-ligase adaptors regulate endocytosis and protein turnover at the cell surface. *Cell* 135:714–725. <http://dx.doi.org/10.1016/j.cell.2008.09.025>.
95. Nagiec MJ, Dohlman HG. 2012. Checkpoints in a yeast differentiation pathway coordinate signaling during hyperosmotic stress. *PLoS Genet* 8:e1002437. <http://dx.doi.org/10.1371/journal.pgen.1002437>.
96. Bilsland-Marchesan E, Arino J, Saito H, Sunnerhagen P, Posas F. 2000. Rck2 kinase is a substrate for the osmotic stress-activated mitogen-activated protein kinase Hog1. *Mol Cell Biol* 20:3887–3895. <http://dx.doi.org/10.1128/MCB.20.11.3887-3895.2000>.
97. Seaman MN, Marcusson EG, Cereghino JL, Emr SD. 1997. Endosome to Golgi retrieval of the vacuolar protein sorting receptor, Vps10p, requires the function of the VPS29, VPS30, and VPS35 gene products. *J Cell Biol* 137:79–92. <http://dx.doi.org/10.1083/jcb.137.1.79>.
98. Seaman MN, McCaffery JM, Emr SD. 1998. A membrane coat complex essential for endosome-to-Golgi retrograde transport in yeast. *J Cell Biol* 142:665–681. <http://dx.doi.org/10.1083/jcb.142.3.665>.
99. Cullen PJ, Sprague GF, Jr. 2012. The regulation of filamentous growth in yeast. *Genetics* 190:23–49. <http://dx.doi.org/10.1534/genetics.111.127456>.
100. Ohya Y, Qadota H, Anraku Y, Pringle JR, Botstein D. 1993. Suppression of yeast geranylgeranyl transferase I defect by alternative prenylation of two target GTPases, Rho1p and Cdc42p. *Mol Biol Cell* 4:1017–1025. <http://dx.doi.org/10.1091/mbc.4.10.1017>.
101. Mack D, Nishimura K, Dennehey BK, Arbogast T, Parkinson J, Toh-e A, Pringle JR, Bender A, Matsui Y. 1996. Identification of the bud emergence gene *BEM4* and its interactions with rho-type GTPases in *Saccharomyces cerevisiae*. *Mol Cell Biol* 16:4387–4395.
102. Zarrinpar A, Bhattacharyya RP, Nittler MP, Lim WA. 2004. Sho1 and Pbs2 act as scaffolds linking components in the yeast high osmolarity MAP kinase pathway. *Mol Cell* 14:825–832. <http://dx.doi.org/10.1016/j.molcel.2004.06.011>.
103. Tatabayashi K, Yamamoto K, Tanaka K, Tomida T, Maruoka T, Sakakawa E, Saito H. 2006. Adaptor functions of Cdc42, Ste50, and Sho1 in the yeast osmoregulatory HOG MAPK pathway. *EMBO J* 25:3033–3044. <http://dx.doi.org/10.1038/sj.emboj.7601192>.
104. Truckses DM, Bloomekatz JE, Thorner J. 2006. The RA domain of Ste50 adaptor protein is required for delivery of Ste11 to the plasma membrane in the filamentous growth signaling pathway of the yeast *Saccharomyces cerevisiae*. *Mol Cell Biol* 26:912–928. <http://dx.doi.org/10.1128/MCB.26.3.912-928.2006>.
105. Katzmann DJ, Sarkar S, Chu T, Audhya A, Emr SD. 2004. Multivesicular body sorting: ubiquitin ligase Rsp5 is required for the modification and sorting of carboxypeptidase S. *Mol Biol Cell* 15:468–480.
106. Swidergall M, van Wijlick L, Ernst JF. 2015. Signaling domains of mucin Msb2 in *Candida albicans*. *Eukaryot Cell* 14:359–370. <http://dx.doi.org/10.1128/EC.00264-14>.
107. Herrero de Dios C, Roman E, Diez C, Alonso-Monge R, Pla J. 2013. The transmembrane protein Opy2 mediates activation of the Cek1 MAP kinase in *Candida albicans*. *Fungal Genet Biol* 50:21–32. <http://dx.doi.org/10.1016/j.fgb.2012.11.001>.
108. Roman E, Cottier F, Ernst JF, Pla J. 2009. Msb2 signaling mucin controls activation of Cek1 mitogen-activated protein kinase in *Candida albicans*. *Eukaryot Cell* 8:1235–1249. <http://dx.doi.org/10.1128/EC.00081-09>.
109. Roman E, Nombela C, Pla J. 2005. The Sho1 adaptor protein links oxidative stress to morphogenesis and cell wall biosynthesis in the fungal pathogen *Candida albicans*. *Mol Cell Biol* 25:10611–10627. <http://dx.doi.org/10.1128/MCB.25.23.10611-10627.2005>.
110. Boissnard S, Ruprich-Robert G, Florent M, Da Silva B, Chapeland-Leclerc F, Papon N. 2008. Role of Sho1p adaptor in the pseudohyphal development, drug sensitivity, osmotolerance, and oxidant stress adaptation in the opportunistic yeast *Candida lusitanae*. *Yeast* 25:849–859. <http://dx.doi.org/10.1002/yea.1636>.
111. Perez-Nadales E, Di Pietro A. 2014. The transmembrane protein Sho1 cooperates with the mucin Msb2 to regulate invasive growth and plant infection in *Fusarium oxysporum*. *Mol Plant Pathol* 16:593–603. <http://dx.doi.org/10.1111/mpp.12217>.
112. Levin DE. 2011. Regulation of cell wall biogenesis in *Saccharomyces cerevisiae*: the cell wall integrity signaling pathway. *Genetics* 189:1145–1175. <http://dx.doi.org/10.1534/genetics.111.128264>.
113. Yang X, Mao F, Lv X, Zhang Z, Fu L, Lu Y, Wu W, Zhou Z, Zhang L, Zhao Y. 2013. *Drosophila* Vps36 regulates Smo trafficking in Hedgehog signaling. *J Cell Sci* 126:4230–4238. <http://dx.doi.org/10.1242/jcs.128603>.
114. Bache KG, Stuffers S, Malerod L, Slagsvold T, Raiborg C, Lechardeur D, Walchli S, Lukacs GL, Brech A, Stenmark H. 2006. The ESCRT-III subunit hVps24 is required for degradation but not silencing of the epidermal growth factor receptor. *Mol Biol Cell* 17:2513–2523. <http://dx.doi.org/10.1091/mbc.E05-10-0915>.
115. Malerod L, Stuffers S, Brech A, Stenmark H. 2007. Vps22/EAP30 in

- ESCRT-II mediates endosomal sorting of growth factor and chemokine receptors destined for lysosomal degradation. *Traffic* 8:1617–1629. <http://dx.doi.org/10.1111/j.1600-0854.2007.00630.x>.
116. Jekely G, Rorth P. 2003. Hrs mediates downregulation of multiple signaling receptors in *Drosophila*. *EMBO Rep* 4:1163–1168. <http://dx.doi.org/10.1038/sj.embor.7400019>.
  117. Teis D, Saksena S, Judson BL, Emr SD. 2010. ESCRT-II coordinates the assembly of ESCRT-III filaments for cargo sorting and multivesicular body vesicle formation. *EMBO J* 29:871–883. <http://dx.doi.org/10.1038/emboj.2009.408>.
  118. Vaccari T, Bilder D. 2005. The *Drosophila* tumor suppressor vps25 prevents nonautonomous overproliferation by regulating notch trafficking. *Dev Cell* 9:687–698. <http://dx.doi.org/10.1016/j.devcel.2005.09.019>.
  119. Calebiro D, Nikolaev VO, Persani L, Lohse MJ. 2010. Signaling by internalized G-protein-coupled receptors. *Trends Pharmacol Sci* 31: 221–228. <http://dx.doi.org/10.1016/j.tips.2010.02.002>.
  120. Finger FP, Novick P. 2000. Synthetic interactions of the post-Golgi mutations of *Saccharomyces cerevisiae*. *Genetics* 156:943–951.
  121. Ryan O, Shapiro RS, Kurat CF, Mayhew D, Baryshnikova A, Chin B, Lin ZY, Cox MJ, Vizeacoumar F, Cheung D, Bahr S, Tsui K, Tebbji F, Sellam A, Istel F, Schwarzmuller T, Reynolds TB, Kuchler K, Gifford DK, Whiteway M, Giaever G, Nislow C, Costanzo M, Gingras AC, Mitra RD, Andrews B, Fink GR, Cowen LE, Boone C. 2012. Global gene deletion analysis exploring yeast filamentous growth. *Science* 337:1353–1356. <http://dx.doi.org/10.1126/science.1224339>.